Ligand-functionalized nanoparticles for chemo- and stereoselective, heterogeneous catalysis

Dissertation

zur Erlangung des Doktorgrades der Naturwissenschaften

- Dr. rer. nat. -

des Fachbereichs 2 (Biologie/ Chemie)

der Universität Bremen

Universität Bremen*
*EXCELLENT.

vorgelegt von

Imke Schrader

geboren in Bremen

Bremen, 16. Februar 2017

Die hier vorliegende Arbeit wurde im Zeitraum von Dezember 2013 bis Februar 2017 unter der Leitung von Herrn Dr. Sebastian Kunz in der Arbeitsgruppe von Herrn Prof. Dr. Marcus Bäumer am Institut für Angewandte und Physikalische Chemie (IAPC) der Universität Bremen durchgeführt.

1. Gutachter: Dr. Sebastian Kunz
2. Gutachter: Prof. Dr. Dieter Wöhrle

Tag des Kolloquiums: 25.04.2017

Selbstständigkeitserklärung

Hiermit erkläre ich, dass ich die Doktorarbeit mit dem Titel *Ligand-functionalized nanoparticles for chemo- and stereoselective, heterogeneous catalysis* selbstständig verfasst und geschrieben habe und außer den angegebenen Quellen keine weiteren Hilfsmittel verwendet habe.

Ebenfalls erkläre ich hiermit, dass es sich bei den von mir abgegebenen Arbeiten um drei identische Exemplare handelt.

(Imke Schrader)

Bremen, 16. Februar 2017

Mein großer Dank geht an …

… **Dr. Sebastian Kunz** für die Bereitstellung dieses interessanten Themas und die damit verbundenen Herausforderungen. Außerdem danke ich ihm für die hervorragende Betreuung, die tolle Zusammenarbeit, sein stetiges Interesse, seine wissenschaftliche Diskussionsbereitschaft und seine Unterstützung bei jeglichen Fragen. Und zu guter Letzt danke ich ihm für die köstlichen Weihnachtsfeiern.

… **Prof. Dr. Marcus Bäumer** für die Ermöglichung meiner Arbeit, die Unterstützung während meiner Promotion und die tolle Zeit am IAPC.

… **Cornelia Rybarsch-Steinke** und **Martin Nowak** für ihren vielfältigen Einsatz und ihre Unterstützung. Ohne euch wäre vieles nicht möglich gewesen!

… **Dr. habil. Vladimir Azov** für die fachliche Unterstützung und die organische Sicht auf mein Thema.

… **Jana Backenköhler** für die Einführung in dieses Thema, die vielen gemeinsamen Stunden im Labor und die Aufnahme von NMR-Spektren. Als „Team“ waren wir unschlagbar.

… **Dr. Jonas Warneke** für die Aufnahme von NMR-Spektren, die Unterstützung bei der Auswertung und die Hilfe bei der Erstellung meiner Publikationen.

… **Dr. Eva Morsbach** und **Dr. Miriam Klink** für die gemeinsamen Jahre im Labor und Büro.

… **Dr. Andreas Schaefer** für die Hilfe bei den IR-Messungen und die stetige Unterstützung und angenehmen Pausen.

… **Sarah Neumann und Anastasia Lackmann** für die fachliche Unterstützung, die Aufnahmen am TEM und die Messungen am GC-MS. Aber natürlich viel mehr für die Ablenkung in den morgendlichen Kaffeepausen, während des Mittagessens und in der Freizeit.

… die weiteren Mitglieder und ehemaligen Mitglieder der **AG Bäumer** für die freundliche Arbeitsatmosphäre, das gute Arbeitsklima, für die anregenden Diskussionen, die gute Zusammenarbeit und die Hilfsbereitschaft.

… meine **Forschungspraktikanten** für die Hilfe bei der Erstellung der Ergebnisse.

… meine **Familie** für die seelische Unterstützung, offene Ohren und Ablenkung bei jeglichen schwierigen Phasen.

… meinen **Freund Anatol** für seine Geduld, sein Interesse und seine Unterstützung. Danke, dass du immer für mich da bist!

List of Publications

Die hier vorliegende Dissertation wurde auf Grundlage von Publikation [2], [3], [4] und [5] erstellt. Eine vollständige Publikationsliste befindet sich im Anhang.

[I] S. Kunz, M. M. Maturi, I. Schrader, J. Backenköhler, M. Tschurl, U. Heiz "Same Ligand – Different Binding Mode: A Way to Control the Binding of N-acetyl-cysteine (NAC) to Pt Clusters" *Journal of Colloid and Interface Science*, **2014**, *426*, 264-269.

[II] I. Schrader, J. Warneke, J. Backenköhler, S. Kunz "Functionalization of Platinum Nanoparticles with L-Proline: Simultaneous Enhancement of Catalytic Activity and Selectivity" *Journal of the American Chemical Society,* **2015***, 137,* 905-912.

[III] I. Schrader, J. Warneke, S. Neumann, S. Grotheer, A. Abildgaard Swane, J. J. K. Kirkensgaard, M. Arenz, S. Kunz "Surface Chemistry of "Unprotected" Nanoparticles: A Spectroscopic Investigation on Colloidal Particles" *The Journal of Physical Chemistry C*, **2015**, *119*, 17655-17661.

[IV] I. Schrader, S. Neumann, R. Himstedt, A. Zana, J. Warneke, S. Kunz "The Effect of Particle Size and Ligand Configuration on the Asymmetric Catalytic Properties of Proline-functionalized Pt-nanoparticles" *Chemical Communications*, **2015**, *51*, 16221-16224.

[V] I. Schrader, S. Neumann, A. Sulce, F. Schmidt, V. Azov, S. Kunz "Asymmetric Heterogeneous Catalysis – Transfer of Molecular Principles to Nanoparticles by Ligand Functionalization", **2017**, *submitted*.

[VI] S. Neumann, S. Grotheer, J. Tielke, I. Schrader, J. Quinson, A. Zana, M. Oezaslan, M. Arenz, S. Kunz "Nanoparticles in a Box: A Concept to Isolate, Store and Re-Use Colloidal Surfactant-Free Precious Metal Nanoparticles" **2017**, *submitted*.

Die oben genannten Publikationen sind im Rahmen intensiver Zusammenarbeit mit Kollegen aus verschiedenen Arbeitsgruppen und Universitäten entstanden. Im Folgenden wird mein eigener Anteil an den aufgeführten Publikationen erläutert:

Publikation I: Bei dieser Publikation beschränkt sich mein Anteil auf die Präparation der Proben für die NMR-Messungen, die Durchführung dieser Messungen, wissenschaftliche Diskussionen sowie das Korrekturlesen des Manuskriptes.

Publikation II: Für diese Publikation lagen die Probenpräparation, die Durchführung der Katalyse-Experimente, die Analyse der Katalyse-Experimente mittels GC, die Interpretation der Ergebnisse sowie das Verfassen des Manuskripts in meiner Verantwortung. Dr. Jonas Warneke führte die NMR-Messungen durch und übernahm die Interpretation dieser Daten. Jana Backenköhler lieferte erste Ergebnisse für diese Publikation im Rahmen eines Forschungspraktikums. Dr. Sebastian Kunz hat die Planung, die Diskussion und das Schreiben begleitet. Conny Rybarsch-Steinke übernahm die Durchführung der AAS-Messungen. Die EA-Messungen wurden von Caroline Zeiser durchgeführt. Dr. Eva Morsbach hat die TEM-Messungen durchgeführt. Dr. Arne Wittstock führte die GC-MS Messungen durch.

Publikation III: Für diese Publikation lagen die Synthese, die IR-spektroskopische Charakterisierung, die Diskussion der Ergebnisse sowie das Verfassen des Manuskripts in meiner Verantwortung. Dr. Jonas Warneke hat die NMR- und MS- Messungen durchgeführt und die Auswertung dieser Daten übernommen. Sarah Neumann und Sarah Grotheer lieferten Beiträge zur Synthese und Charakterisierung. Die SAXS-Messungen wurden von Jacob J. K. Kirkensgaard durchgeführt und er lieferte Beitrage zur Diskussion dieser Daten. Andreas Abildgaard Swane hat Vergleichsproben für die SAXS-Messungen hergestellt. Dr. Matthias Arenz übernahm die Diskussion der SAXS Daten. Dr. Sebastian Kunz hat die Planung, die Diskussion und das Schreiben begleitet.

Publikation IV: Für diese Publikation lagen die Probenpräparation, die Durchführung der Katalyse-Experimente, die Analyse der Katalyse-Experimente mittels GC, die Interpretation der Ergebnisse, die IR-Messungen sowie das Verfassen des Manuskripts in meiner Verantwortung. Sarah Neumann und Rieke Himstedt lieferten Beiträge zu den Katalyse-Experimenten. Dr. Alessandro Zana führte die TEM-Messungen durch. Dr. Jonas Warneke hat die MS-Messungen durchgeführt. Dr. Sebastian Kunz hat die Planung, die Diskussion und das Schreiben begleitet. AAS- und EA-Messungen wurden an der TU München durchgeführt.

Publikation V: Für diese Publikation lagen die Planung, die Probenpräparation, die Durchführung der Katalyse-Experimente, die Analyse der Katalyse-Experimente mittels GC, die Interpretation der Ergebnisse sowie das Verfassen des Manuskripts in meiner Verantwortung. Anda Sulce ergänzte diese Publikation mit der von ihr durchgeführten Hydrierung von Ethyl 3-oxo-3-phenylpropanoat. Fabian Schmidt hat im Rahmen eines Forschungspraktikums (unter meiner Betreuung) und Sarah Neumann im Rahmen einer Masterarbeit erste Ideen für diese Publikation geliefert. Dr. Vladimir Azov hat zur Diskussion beigetragen. Dr. Sebastian Kunz hat die Planung, die Diskussion und das Schreiben begleitet. Conny Rybarsch-Steinke übernahm die Durchführung der AAS-Messungen.

Publikation VI: Bei dieser Publikation beschränkt sich mein Anteil auf synthetische Beiträge, wissenschaftliche Diskussionen sowie das Korrekturlesen des Manuskriptes.

Deutsche Zusammenfassung

Die asymmetrische Katalyse ist ein zentrales Thema für die Etablierung nachhaltiger chemischer Präparationswege. In den letzten Jahrzehnten wurden hauptsächlich homogene Katalysatoren, die aus einzelnen Metallatomen mit chiralen organischen Liganden bestehen, entwickelt. Ihre Anwendung im industriellen Maßstab ist jedoch, durch die technischen Nachteile hinsichtlich des schlechten Recyclings und der Schwierigkeit kontinuierliche Prozesse zu entwickeln, begrenzt. Eine Alternative ist der Einsatz von chiralen Modifikatoren mit Trägerkatalysatoren. Dieser Ansatz bietet inhärente praktische und technische Vorteile gegenüber homogenen Katalysatoren und wird industriell angewandt. Allerdings ist der Pool von effektiven Modifikatoren sehr begrenzt.

Ein neuartiger Ansatz zur Lösung der Probleme des Modifierkonzepts ist die Funktionalisierung von Trägerkatalysatoren mit chiralen Liganden. Dieses Konzept wurde im Rahmen der vorliegenden Arbeit konsequent untersucht, um unter anderem das Potential ligandenfunktionalisierter Nanopartikel für die asymmetrische Katalyse zu untersuchen. Es wurde ein synthetischer Ansatz genutzt, der die unabhängige Kontrolle der katalytisch relevanten Materialeigenschaften (Partikel, Ligand und Träger) ermöglicht. Stabile kolloidale Nanopartikel (NP) wurden ohne die Verwendung von stark bindenden organischen Stabilisatoren hergestellt. Wie in dieser Arbeit spektroskopisch gezeigt werden konnte, sind derartige Partikel durch CO und OH^- stabilisiert. Da beide Oberflächenspezies leicht durch stärker bindende Moleküle substituiert werden können, werden diese Partikel als "ungeschützte" NP bezeichnet und können als Bausteine für die Herstellung von maßgeschneiderten ligandenfunktionalisierten NP verwendet werden.

NP besitzen per se keine chirale Information. Um eine stereoselektive Hydrierung von prochiralen Reaktanden zu erreichen, muss ein chirales Element eingebracht werden. In dieser Arbeit erwies sich die Verwendung von L-Prolin (PRO) als Ligand als besonders effektiv. Die erfolgreiche Bindung von PRO an die Partikeloberfläche wurde durch NMR bestätigt. Nach Abscheidung auf Al_2O_3 wurden die geträgerten ligandenfunktionalisierten NP zunächst als Trägerkatalysator für die Hydrierung von Acetophenon eingesetzt. Katalytische Untersuchungen zeigten, dass PRO-Pt-NP im Vergleich zu „ligandenfreien" Pt-NP exzellente Chemoselektivitäten für die Hydrierung

der Carbonylgruppe liefern. Es wurde vermutet, dass durch die Bindung von PRO an die Metalloberfläche Oberflächenatome blockiert und Ensembles von benachbarten Oberflächenatomen verdünnt werden. Dies unterdrückt die unerwünschte Hydrierung des Phenylrings. Trotz des Blockens von Oberflächenatomen durch Liganden wurde festgestellt, dass die Reaktionsrate erhöht war, wenn „ligandenfreie" NP mit PRO funktionalisiert werden. Diese Zunahme der Aktivität konnte nicht auf das Verdünnen großer Ensembles zugunsten von kleinen zurückgeführt werden. Stattdessen wurde das Auftreten eines Mechanismus, der aus der homogenen Katalyse als „N-H-Effekt" bekannt ist, geschlussfolgert. Der Wasserstoff-Substituent an der Aminogruppe von PRO wird nach Bindung an Pt acide. Dieses Proton aktiviert die C=O-Gruppe des Reaktanden, was zu einem alternativen Reaktionsweg mit einer erhöhten Rate gegenüber der rein metallkatalysierten Reaktion führt.

Die Hydrierung von Acetophenon mit PRO-Pt-NP ergab einen relativ niedrigen Enantiomerenüberschuss (ee) von 14%. Eine signifikante Verbesserung zu 34% ee wurde durch die Änderung der Reaktion auf die Hydrierung von Ethylacetoacetat (EAA) erreicht. Dieser Wert war ausreichend hoch, um den Einfluss der Partikelgröße und der Ligandenkonfiguration auf die katalytischen Eigenschaften zu untersuchen. Es konnte gezeigt werden, dass die Partikelgröße nur die Aktivität, nicht aber die Stereoselektivität verändert. Auch die Ligandenkonfiguration hatte keinen Einfluss auf den Absolutwert des ees. Dies lässt schlussfolgern, dass die Stereoselektivität nicht von der Partikelgröße abhängt, sondern primär durch die Ligand-Reaktand-Wechselwirkung bestimmt wird.

Um die Ligand-Reaktand-Wechselwirkung näher zu untersuchen und die Stereoselektivitäten zu verbessern, wurde eine Struktur-Aktivitäts-, Struktur-Selektivitätsstudie durchgeführt. Durch Variation von Ligand und Reaktand konnte gezeigt werden, dass die Kombination einer α-Aminosäure und eines β-Ketoesters in einer stabilisierten 2-Punkt-Bindung resultiert, die zu einer verstärkten stereoselektiven Kontrolle führt. Die Anwendung von Grundprinzipien der asymmetrischen homogenen Katalyse auf dieses Modell führte zu einer Erhöhung des ees auf 73% durch rationale Reaktandenwahl.

Die in dieser Arbeit vorgestellten Ergebnisse zeigen die Fähigkeit, Prinzipien von der homogenen zur heterogenen Katalyse zu übertragen durch die Funktionalisierung von NP mit chiralen Liganden. Auf diese Weise können hoch chemo- und stereoselektive,

sowie stabile Katalysatoren entworfen werden. Während in der heterogenen Katalyse Selektivitätsverbesserungen in der Regel von einem Aktivitätsverlust begleitet werden, wurde gezeigt, dass die Verwendung von Liganden eine gleichzeitige Verbesserung der Aktivität und Selektivität ermöglicht. Die Anwendung von Liganden für geträgerte Katalysatoren dient somit als neuer Ansatz mit bisher unbekanntem Potential, um die katalytische Leistung von heterogenen Katalysatoren abzustimmen.

English Abstract

Asymmetric catalysis is an important topic for establishing sustainable chemical preparation routes. Mainly homogeneous catalysts consisting of single metal atoms with chiral organic ligands have been developed within the past decades, but their application on an industrial scale is limited due to practical disadvantages. An alternative concept is the use of chiral modifiers in combination with supported metal catalysts. This approach offered inherent practical and technical advantages over homogeneous catalysts and reached industrial maturity. However, the pool of effective modifiers is very limited. Considering the progress achieved within the last years and the vast amount of manuscripts on this topic, industrial experts question the ability to achieve further breakthroughs for chiral modifiers.

The functionalization of supported metal nanoparticles (NPs) with chiral, hydrophilic ligands and their use as asymmetric heterogeneous catalysts is a novel approach, exhibiting the potential to bridge the gap between homogeneous and heterogeneous catalysis. Within this project, highly active and selective heterogeneous catalysts were developed based on ligand-functionalized Pt NPs. The materials were prepared by a stepwise rational design approach. “Unprotected” Pt NPs (1-2 nm), which were demonstrated to be stabilized by CO and OH^-, were used as a building block to prepare ligand-functionalized NPs and via deposition of these particles onto support materials heterogeneous catalysts were obtained. This preparation concept allows for independent control over particle, ligand, and support properties.

Previous studies on the functionalization of these “unprotected” Pt NPs with thiol ligands showed a drastic decrease in activity and low stereoselectivities. To approach the activity challenge only amine ligands were used in this study, specifically L-proline (PRO). The hydrogenation of acetophenone, used as test reaction, revealed that Pt NPs could be tuned to be 100% chemoselective at enhanced catalytic activity upon functionalization with PRO. This unexpected finding could be related to a ligand-acceleration effect known from homogeneous catalysis that is transferred onto NPs when using PRO as a ligand.

By switching to β-ketoesters as reactants first significant improvements in stereoselectivity were obtained (enantiomeric excess (ee) over 30%). It was demonstrated that the product configuration could be controlled by the ligand

configuration. However, more surprising the stereoselectivity of these complex materials does not depend on the particle size. Instead, it is only determined by the ligand-reactant interaction. Based on this knowledge a structure-activity and structure-selectivity study was performed that led to the postulation of a simple ligand-reactant interaction model. The model predicts correctly the stereochemistry of the reaction and the application of general guiding principles from asymmetric homogeneous catalysis to this model allowed to increase the ee up to 73%.

The present work shows the feasibility to transfer molecular principles from homogeneous to heterogeneous catalysts by ligand functionalization. This reveals a yet unexplored potential to tune activity and selectivity of supported catalysts. In particular, this thesis demonstrates that by ligand functionalization one of the greatest selectivity challenges in heterogeneous catalysis can be addressed: asymmetric catalysis.

Contents

List of Abbreviations

AAS	**A**tomic **A**bsorption **S**pectroscopy
ACAC	**Ac**etyl**ac**etone
ACE	**A**ngiotensin-**c**onverting-**e**nzyme
ALA	L-**ala**nine
ATR-IR	**A**ttenuated **T**otal **R**eflection - **I**nfra**r**ed
BAA	**B**utyl**a**ceto**a**cetate
BINAP	2,2´-Bis(diphenylphosphino)-1,1´-**binap**hthalene
E-factor	**E**nvironmental-**factor**
EA	**E**lemental **A**nalysis
EAA	**E**thyl**a**ceto**a**cetate
ee	**E**nantiomeric **E**xcess
EG	**E**thylene **G**lycol
EOPP	**E**thyl 3-**o**xo-3-**p**henyl**p**ropanoate
EPA	US **E**nvironmental **P**rotection **A**gency
ESI-MS	**E**lectro**s**pray **I**onization - **M**ass **S**pectrometry
FID	**F**lame **I**onization **D**etector
GC	**G**as **C**hromatograph
HEP	2-**hep**tanone
IPA	**I**so**p**ropyl**a**cetoacetate
IR	**I**nfra**r**ed
L-DOPA	**L**-3,4-**d**ihydr**o**xy**p**henyl**a**lanine
MAA	**M**ethyl**a**ceto**a**cetate
MDOV	**M**ethyl 4,4-**d**imethyl-3-**o**xo**v**alerate
MIBA	**M**ethyl **i**so**b**utyryl**a**cetate
ML	**M**ethyl**l**evulinate

MOH	**M**ethyl 3-**o**xo**h**exanoate
MOHp	**M**ethyl 3-**o**xo**h**e**p**tanoate
MOV	**M**ethyl 3-**o**xo**v**alerate
MP	**M**ethyl**p**yruvat
MPE	4-**m**ethyl-2-**pe**ntanone
NMR	**N**uclear **M**agnetic **R**esonance
NP	**N**ano**p**article
PAA	**P**ropyl**a**ceto**a**cetate
PIP	L-**pip**ecolic acid
PRO	L-**pro**line
SAXS	**S**mall-**a**ngle **X**-ray **s**cattering
SER	L-**ser**ine
TBA	**T**ert-**b**utyl **a**cetoacetate
TEM	**T**ransmission **E**lectron **M**icroscopy
THR	L-**thr**eonine
TOF	**T**urn**o**ver **F**requency
TON	**T**urn**o**ver **N**umber

1. Introduction

While academic chemical research often focusses primarily on yields, the need for environmental friendly preparation routes is a considerable challenge for the chemical industry,[1] as the saving of energy and resources are essential aims for our society. In the beginning of the 1990s, Anastas applied the term “green chemistry” for this task at the US Environmental Protection Agency (EPA).[2-3] At nearly the same time (1992), Roger Sheldon introduced the so-called environmental-factor (E-factor) to quantify the efficiency of chemical processes.[4-5] The E-factor illustrates the need for green chemistry in a simple way. It is defined as the amount of waste in kg generated for the production of 1 kg product (E-factor = kg waste/ kg product). A higher E-factor implies the generation of more waste and thus a more negative environmental impact. Typical E-factors for different chemistry related industrial segments with the corresponding product volumes are shown in Table 1.

Table 1: Production volumes and E-factors of different industrial segments (from [4]).

Industry segment	Product tonnage	E-factor kg waste/ kg product
Oil refining	10^6 – 10^8	<0,1
Bulk chemistry	10^4 – 10^6	<1-5
Fine chemicals	10^2 - 10^4	5-50
Pharmaceuticals	10 - 10^3	25-100

Apparently, both, fine chemistry and pharmaceutical industry, have tremendously high E-factors. Because of that, the total waste generated for a typical product in these industries can be in the same range as that of a bulk chemical, although the production volumes are much smaller.

Main challenges in fine and pharmaceutical chemistry are the control of chemo- and stereoselectivity. Chemoselectivity describes the selective transformation of one functional group in the presence of other reactive moieties. Stereoselectivity relates to the preferential formation of one of two stereoisomers. A specific case of stereoisomers are enantiomers, which behave like mirror images. In general enantiomers exhibit the same chemical and physical properties, but they rotate plane-polarized light to

opposite directions. The biological and thus also the pharmacological activities can, however, differ strongly. In the 1960er, the contergan (thalidomide) scandal has drawn public attention to the relevance of stereochemistry. One enantiomer of thalidomide has the desired sedative effect, but the other one leads to malformation of the limbs of embryos.[6-7] This explains the strong increase of enantiopure products since the late 1980s especially in the pharmaceutical industry (see Fig. 1a). Before, pharmaceutical products were dominated by racemates (50:50 mixture of the two enantiomers) and achiral compounds. However, in the late 1980s, Ariëns pointed out that "as much as it is justified to use a drug with 50% of a presumably harmless impurity because it is difficult to eliminate, so much is it reasonable to accept 50% of a presumably harmless impurity in the form of isomeric ballast".[8] This highlighted the necessity of enantiopure compounds. As a consequence, the regulatory authorities defined more strict requirements on drug discovery[9] and today around 80% of all pharmaceutical ingredients are enantiopure compounds.

Besides the share for enantiopure compounds, also the market for chiral compounds consisting of a single enantiomer increases continuously (see Fig. 1b).[10] This makes improvements of E-factors in this industrial segment even more important.

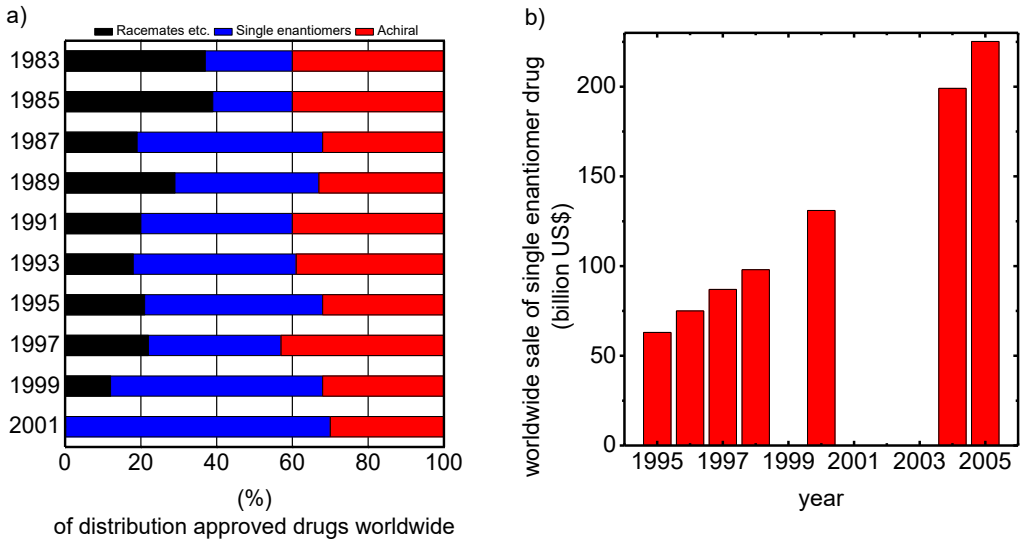

Figure 1: a) Distribution of approved drugs worldwide respectively to their chiral nature (from [11-12]). b) Worldwide sales of single-enantiomer pharmaceutical products (from [13-14]).

There are different ways to receive enantiopure compounds. Today, the most common approach is still the synthesis of the racemate, followed by enantiomeric separation.[15] This allows for explaining in part the high E-factors in fine and pharmaceutical chemistry. Thereby 50% of the undesired enantiomer is produced, and additional

waste, as well as product losses, are generated by the separation of the two enantiomers.[13] The development of effective stereoselective reaction pathways is thus an important topic in chemical research.

One strategy is stereoselective synthesis. An enantiopure chiral auxiliary interacts with a prochiral substrate. This leads to an asymmetric induction within the reactant and results in a diastereoselective reaction pathway. After reaction, the auxiliary has to be cleaved in an additional post-synthetic step, to obtain the pure enantiomer. Such synthesis usually requires an equivalent amount of chiral auxiliary, which has to be purified or discarded afterward, also causing high E-factors.[16] In addition, stereoselective reactions often proceed at low reaction rates. These limitations can be accepted when working on lab-scale synthesis. However, industrial applications require high time to volume yields and low E-factors. This emphasizes the need of catalytic routes with high stereoselectivities to reduce E-factors effectively for chemical conversions in fine and pharmaceutical chemistry.[17] Therefore, concepts to improve state-of-the-art catalyst, as well as the development of new catalytic concepts, are needed.[18]

The control of stereoselectivity has been intensively studied in the field of homogeneous catalysis. A typical chiral homogeneous catalyst is an organic transition metal complex, which is soluble in the reaction medium. The catalyst consists of a metal center, which can activate a reactant by coordination. The presence of chiral organic (usually phosphorus) ligands can induce chirality to the reactant by interacting sterically and electronically with it. This may open asymmetric reaction pathways and lead to stereoselective conversions.[19-21]

The first “man-made” asymmetric homogeneous catalysts were reported in the 1960s. This progress was significantly promoted by the development of the first chiral phosphine ligands.[22] In the beginning of the 1970s, the production of L-3,4-dihydroxyphenylalanine (L-DOPA) introduced by William S. Knowles was the first industrial process.[23] The tremendous progress in asymmetric homogeneous catalysis was honored with the 2001 Nobel Prize in Chemistry that Knowles, Noyori, and Sharpless received for their outstanding contributions in this field.[22, 24]

The activities and selectivities of homogeneous catalysts have been optimized by the development of tailored ligands. Today many homogeneous catalysts are known that allow for achieving enantiomeric excesses (ee) of 99%.[25] Nevertheless, only a very

few are applied on an industrial scale (about 15 status 2005).[15] On the one hand, ligand syntheses are usually very complex leading to high development and production costs. On the other hand, the dissolved catalyst is difficult to separate from the reaction medium. As a result, recycling of the catalyst is a great challenge, and the product mixtures are typically contaminated by poisoning ligands and precious metals.[26] This requires additional purification steps. Furthermore, the solubility of the catalyst greatly limits the possibility to establish continuous processes.[27] These problems explain the limited use of asymmetric homogeneous catalysts in chemical industry.

Another possibility that enables an effective use of precious metals as catalytic materials is the use of heterogeneous catalysts. The “classic” precious metal based heterogeneous catalyst is a supported nanoparticle (NP). These materials can overcome several problems associated with homogeneous catalysis.[28] In contrast, to a homogeneous catalyst, a supported catalyst is not soluble in the reaction medium. Such catalysts can, therefore, be easily handled, separated, and recovered by filtration. This bears significant economic and ecological advantages over homogeneous catalysts.[29] The control of chemo- and stereoselectivity offers, however, a challenging task for supported NPs,[30-31] because they do not have any chiral information.

To develop a resource- and energy- efficient production of enantiopure products, it is thus necessary to combine the advantages of homogeneous catalysts in terms of stereoselectivity with those of heterogeneous catalysts regarding separation and recyclability. This emphasizes the need for stereoselective heterogeneous catalysts.

The idea of combining the advantages of homo- and heterogeneous catalysis led to several approaches, which have been intensively studied in the past. Three of the most prominent concepts are i) the immobilization of homogeneous catalysts,[32] ii) encapsulation into porous materials, and iii) the use of chiral modifiers for supported catalysts.[28]

To make homogeneous catalysis “recyclable”, metalorganic catalysts can be immobilized onto inert supports (see Fig. 2a).

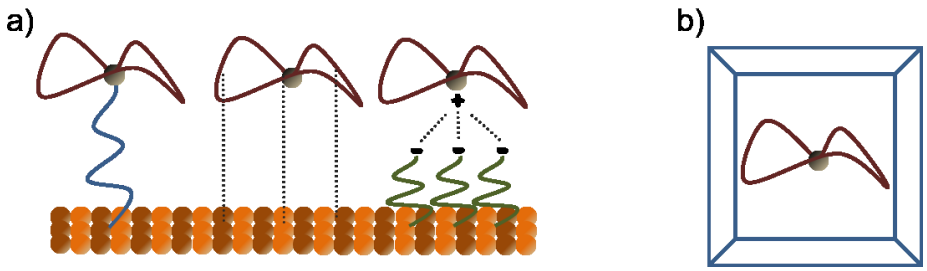

Figure 2: Immobilization of a homogeneous catalyst by interaction with the support (a) or encapsulation in a porous structure (b).

The immobilization can be done by fixation of the catalyst via covalent bonds, adsorption or electrostatic interactions.[32-34] The strength of this approach is that the existing knowledge from homogeneous catalysis can be used. A major problem, however, is that the homogeneous catalyst changes structurally by binding to the carrier. Also, additional chemical modifications must be carried out on the ligand to achieve a binding to the support. This leads to a considerable additional synthesis effort and high costs. Furthermore, structural changes often result in activity and selectivity losses.[35] Another problem can be the stability. The catalysts can detach from the support and the metal can leach into the reaction medium, leading to product contamination and loss of the desired catalytic function.[28] By encapsulating into porous structures (see Fig. 2b),[36] these problems can be partially overcome, but the accessibility of the catalyst is severely restricted, which greatly reduced the catalytic activity.[28, 32]

Although, several scientific examples demonstrate the practicability of immobilization,[34] the approach is yet not been applied on an industrial scale.[32] The main reason is that this approach is economically not feasible because the synthesis of the homogeneous catalysts is expensive and the structural changes, which are necessary to achieve an immobilization require additional preparation steps and costs.[32]

A different approach, motivated now from heterogeneous catalysis, is the use of “chiral modifiers” with supported NPs. Two highly efficient modifier systems with enantioselectivities over 90% are known[37]. The first one is a tartaric acid-modified Raney nickel catalyst (up to 98% ee)[38] and the second one cinchona alkaloid modified Pt (up to 95% ee)[39] (see Fig. 3).

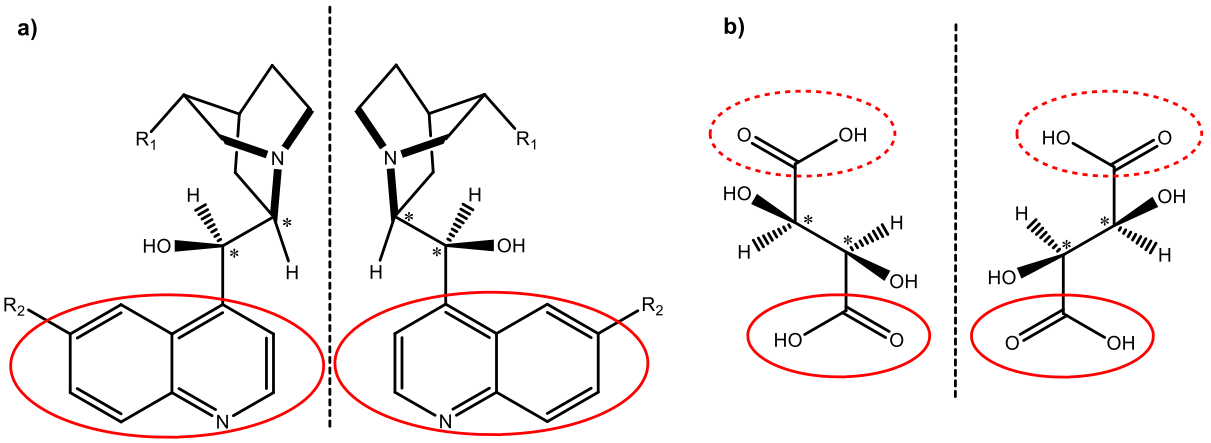

Figure 3: The respectively two chiral forms of cinchona alkaloids (a) and tartaric acid (b). The adsorption on the metal proceeds via the red highlighted part (in tartaric acid one of the highlighted parts will adsorb). The chiral centers are denoted by "". For mechanistic see literature [40-41].*

Chiral modifiers are dissolved in the reaction medium in which a supported NP catalyst is suspended. The modifiers adsorb with one part on the particle surface (red highlighted in Figure 3) and interact with the chiral part (highlighted with *) with the reactant. The latter leads to a chiral induction which is needed for an enantioselective reaction.[40-41] The strength of this approach is that supported NP catalysts can be prepared on a large scale with established methods and the best modifiers are commercially available at moderate costs.[42] The first technical application of a modifier system was the hydrogenation of an α-ketoester, reported by Ciba-Geigy in 1986 with an ee of 80%.[43] This product is a key intermediate for the angiotensin-converting-enzyme (ACE) inhibitor benazepril. Nevertheless, the applicability of modifiers is often limited for the following reasons:

1. Stability of cinchona-based modifiers: the structures of established modifiers are reactive under applied reaction conditions. The aromatic ring (see Fig. 3) is hydrogenated during reaction, leading to a change in adsorption geometry.[44] As a result, the probability for the desired modifier-reactant interaction decreases.
2. Stability of the tartaric acid modifier: the metal tends to leach into the reaction medium.[45-46]
3. Robustness of the tartaric acid modifier system: the catalytic results depend on various parameters (composition of Ni-Al alloy,[46] impregnation/modification procedure (washing, pH, temperature, time, concentration, co-modifier),[38, 46]

reaction conditions (solvent, temperature, pressure)).[47] For this reason, reproducibility is a great challenge for the tartaric acid system.

4. Solubility of the modifier: this prevents the ability to implement a continuous process, as the modifier is purged out of the reactor together with the product stream.[48] Additionally, the modifier stands in an adsorption-desorption equilibrium. This means that free metal surface sites are formed during reaction due to modifier desorption. This is highly undesired as they catalyze unselective side reactions. The stereoselectivity is thus determined by the ratio of modified to unmodified sites and the according reaction rates over these catalytic sites. Therefore, high ees are usually only obtained if the modifier induces a significant enhancement of the reaction compared to the bare metal reaction.[44, 49] This limits the modifier approach to a very few reactant-modifier combinations.

In the following, a novel approach for asymmetric catalysis is introduced that tries to solve some of the limitations of the modifier concept.

2. Functionalization of NPs with Ligands – The Research Concept

The needs to overcome the limitations of the previously described modifier concept are:

1. The chiral source should only contain functional groups which are not reactive under hydrogenation conditions. This requirement excludes groups like C=C, and C=O.
2. The chiral source should be strongly fixed to the surface under catalytic conditions like a ligand in homogeneous catalysis. This allows to suppress the formation of free surface atoms that would cause unselective side reactions.

Based on these conclusions the here introduced approach deals with the functionalization of NPs via binding chiral ligands to the particle surface. At first sight, it seems intuitive to use ligand structures that are known from homogeneous catalysis to be effective for stereoselective conversions e.g. 2,2´-Bis(diphenylphosphino)-1,1´-binaphthalene (BINAP) (see Fig. 4). However, this idea is not feasible, because the

solubility of the ligand in the reaction medium is a crucial aspect for this approach. As most organic reactants are nonpolar, also the solvent has to be nonpolar to ensure solubility of the reactant. The same holds for most ligand structures used in homogeneous catalysis because the ligands have to facilitate the solubility of the metalorganic complex in the reaction medium. If such ligands are bound to a NP they fulfill the same function so that the particles are dispersible in nonpolar media.[50]

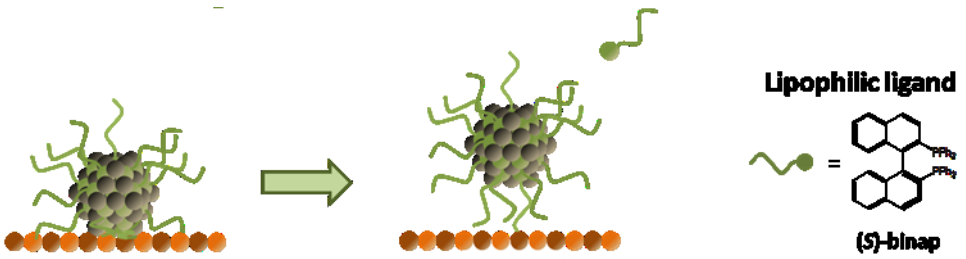

Figure 4: Supported NPs functionalized with a lipophilic ligand (for example BINAP). During reaction in a nonpolar organic solvent, the particle can desorb from the support or/and the ligand from the particle surface.

This means that during a catalytic reaction the NPs can desorb from the support when being functionalized with nonpolar ligands. The particle thus acts as a "quasi-homogeneous" catalyst and the benefit of a supported catalyst is lost. In addition, depending on the binding strength between ligand and metal, the ligand can desorb from the particle surface, and a purely metal catalyzed unselective reaction can proceed. Nonpolar ligands are, therefore, not suitable for applications in heterogeneous catalysis.

To overcome the problems mentioned above, in this work NPs were exclusively functionalized with hydrophilic ligands for catalytic applications in nonpolar solvents (see Fig. 5). Only in this way supported ligand-functionalized NPs remain supported under reaction conditions.

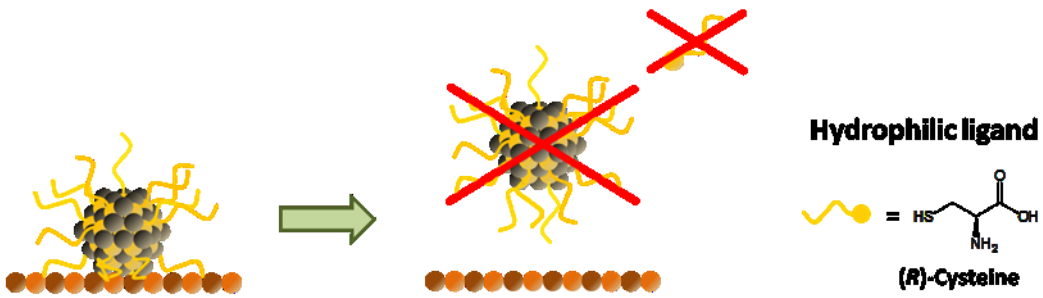

Figure 5: Supported NPs functionalized with a hydrophilic ligand (for example cysteine). During reaction in a nonpolar organic solvent, the particle did not desorb from the support or/and the ligand from the particle surface.

Having opposite solubility properties for the ligand and the solvent inhibit the appearance of strong attractive interactions between the ligand shell and the reaction medium.[51] As a result, neither the NPs desorb from the support nor the ligands from the particle surface. A further benefit of using hydrophilic ligands is that amino acids and corresponding derivatives can be used, which are harmless, cheap and enantiopure available.

To explore the use of hydrophilic ligands for catalytic NPs, the parameters which influence the catalytic properties (activity, selectivity, stability) have to be known. Based on the knowledge from homogeneous and heterogeneous catalysis four parameters have been identified that primarily determine the catalytic performance of supported ligand-functionalized NPs:[52] the particle, the ligand, the support, and the reaction parameters (see Fig. 6).

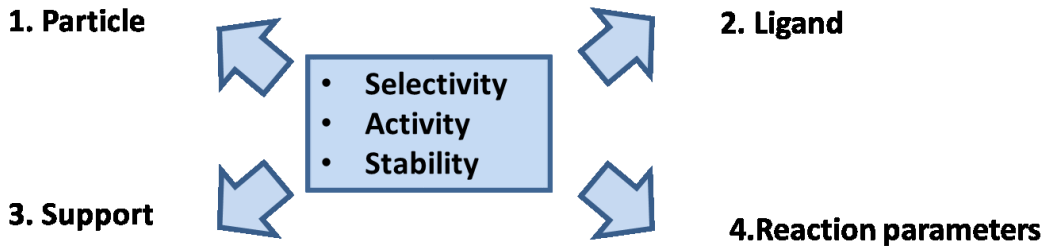

Figure 6: Four parameters which determine primary the catalytic performance of supported ligand-functionalized nanoparticles.

To investigate the influence of these parameters systematically their independent control is a prerequisite. In contrast to the reaction parameters, the material parameters (particle, ligand, and support) cannot be synthesized and controlled independently by conventional preparation routes (e.g. incipient wetness impregnation).[53] In this method, a metal precursor solution is added to a support. The particles are then generated by a reductive treatment on the support. Because the surface chemistry of the support influences the particle generation (particle size), this method prevents that support and particle can be tuned independently.

An alternative route for the preparation of NPs is the colloidal approach.[54] Metal precursors are reduced in a solvent which leads to nucleation followed by particle growth, as proposed by LaMer.[55-56] By tuning the reaction conditions, particles of a given metal and size can be synthesized and subsequently be deposited onto any desired support material. In this work a specific route has been applied that,

furthermore, allows for selective binding of specific ligands.[51] First colloidal NPs are formed in basic ethylene glycol (EG) (step 1, Fig. 7). These formed NPs are called "unprotected" because no organic surfactants are necessary for their stabilization in the reaction medium. By lowering the pH value (1 M HCl) these NPs are precipitated, washed with HCl (step 2), and redispersed in a polar organic solvent (e.g. acetone or cyclohexanone) (step 3). For the functionalization with ligands an alkaline hydrophilic ligand solution is added (step 4). During proper mixing of the two immiscible phases (step 5) a phase transfer reaction takes place. The ligands bind to the particle surface, and the functionalized particles transfer into the aqueous phase. Finally, these ligand-functionalized particles can be deposited in an additional independent step on any desired support (step 6). During all these steps the particle size is maintained as verified by TEM analysis.[51]

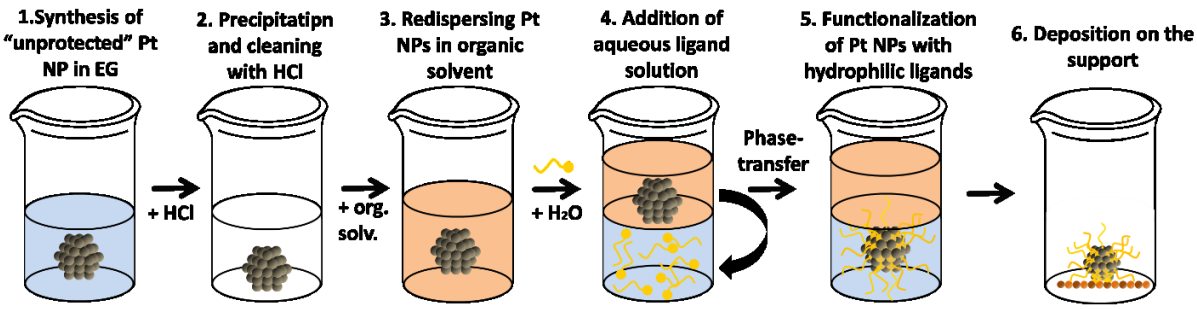

Figure 7: Preparation procedure for the synthesis of ligand-functionalized NPs. First "ligand-free" NPs are synthesis (step 1). This NPs were precipitated and washed with HCl (step 2) and redispersed in an organic solvent (step 3). After addition of a ligand solution (step 4) the particles were functionalized upon proper mixing (step 5). Finally, these particles can be deposited on a support (step 6).

The separation of particle synthesis, functionalization, and deposition enables to vary the most important material properties independently, as illustrated in Figure 8. The applied preparation and reaction route allows independent control over i) the metal and particle size, ii) the functionalizing ligand, and iii) the support. The catalyst prepared by this protocol can then be studied under different reaction conditions (control of reaction parameters). As a result, the influence of the four catalytically most relevant parameters (see Fig. 6) on the activity, selectivity, and stability can be investigated systematically, and changes can be related exclusively to the influence of a single material property or the reaction parameters.

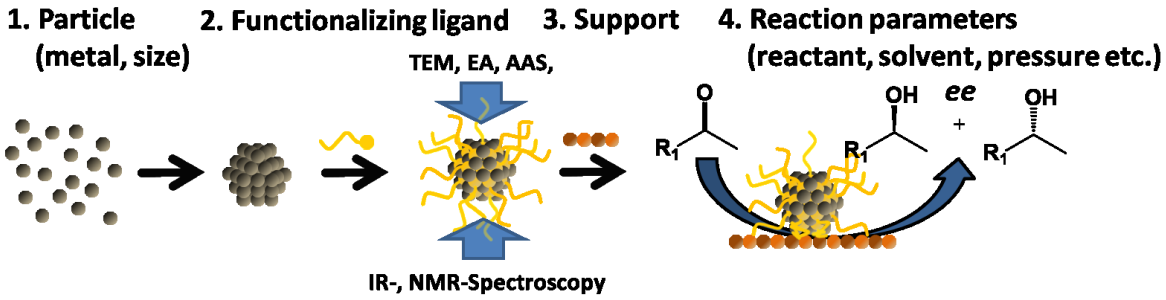

Figure 8: The colloidal approach allows the independent control of different particles (metals and size, 1), the functionalization with different ligands and the characterization with varied methods (2), the deposition on different supports (3), and the variation of the reaction parameters (4). Reproduced from Ref. 51 with permission from the PCCP Owner Societies.

3. Aim of the Work

The aim of this project was to explore the use of hydrophilic ligands for catalytic NPs to determine guidelines for developing novel, highly active and selective catalytic systems. To tackle this challenge the preparation strategy described above (see Fig. 7) for the independent control of the material properties was applied. Although the approach had been established previously, the surface chemistry of the "unprotected" NPs that are used as a building block for the ligand-functionalized NPs (see. Fig. 7) remained unclear. As the particle properties are of essential importance for the catalytic performance (see Fig. 6) the first aim was thus to elucidate their surface chemistry and to achieve a fundamental understanding of these particles.

The ligand was identified as an important parameter that determines the catalytic properties of ligand-functionalized particles (see Fig. 6). It was already shown that "ligand-free" Pt NPs can be functionalized with thiol ligands. However, these ligands showed a strong decrease in activity compared to "ligand-free" Pt NPs and very low ees (ee < 10%). While these results demonstrated the feasibility of using ligands for supported NPs and the preparation concept introduced above (see Fig. 7), they indicated significant disadvantages for the use of thiol ligands in particular their strong poisoning effect. For this reason, the aim of the present work was to investigate amines as a different class of ligands for catalytic NPs, as amines have been previously demonstrated to cause no strong poisoning.[57]

An essential challenge of this project was to shed light onto the ability of ligands to control the selectivity of NPs. In the first step, it was tried to control mainly

chemoselectivity. In the second step, the focus was stereoselectivity to achieve a fundamental understanding for the asymmetric bias of these novel systems and elucidate strategies to obtain high stereoselectivities.

4. Synthesis and Surface Chemistry of "Unprotected" Nanoparticles

4.1 Synthesis of Stable Colloidal Metal NPs

NPs can be synthesized with the "top-down" and the "bottom-up" approach.[50, 55] The "top down" approach uses physical methods such as grinding or sputtering techniques to downsize the bulk material. Thus prepared particles are, however, usually large in size, and the approach exhibits very limited size control.[55] For catalytic investigations, the "bottom-up" approach is in most cases beneficial over physical methods. Single atoms grow to NPs in a wet-chemical synthesis. This is typically achieved by chemical reduction of metal salts.[50] The most commonly used method is the alcohol reduction. The metal precursor is dissolved in an alcohol that acts simultaneously as the solvent and the reduction agent. The concentration of reduced atomic monomers constantly increases until the nucleation starts, which is followed by the growth of the particles as long as precursor is available. Thus formed colloids have a high surface to bulk ratio and tend to minimize their free surface energy by sintering. To prevent sintering stabilizers are added which lower the surface energy of the NPs and shield their surface. Stabilizers are usually added during synthesis and involved in the determination of size and structure.[50]

The main concepts for the stabilization of the colloids are:

1. The electrostatic stabilization by adsorbed ions:[50] ionic compounds in the solution can form an electrical double layer on the metal surface, leading to a coulombic repulsion between the nanoparticles and an electrostatic stabilization.
2. Steric stabilization by macromolecules and ligands:[58] through the binding (covalent or coordinative) of macromolecules (polymers) or ligands[59-60] to the particle surface, a protection layer is formed around the particle that causes a steric shielding.

3. The electrosteric stabilization by surfactants:[58] a combination of electrostatic and steric stabilization can be achieved by the use of ionic surfactants, which have a polar head group that generates an electrical double layer and a lipophilic side chain that provides steric repulsion.
4. The stabilization in dendrimers or micelles:[58, 61-62] NPs can be encapsulated within a dendrimer or a micelle. They form a membrane-like structure around the NP that protects the NPs against sintering.

The protection agents block and hinder the accessibility of the surface. This allows to suppress sintering. For catalytic applications, they, however, have to be removed, if the aim is to study the catalytic properties of the bare metal surface. Organic stabilizers can be removed by solvent extraction, oxidative heat or oxidative low-temperature treatments. However, such treatments can irreversibly alter the particle properties, which diminishes the benefit of a colloidal route.[63-64] An alternative strategy that allows overcoming these problems is discussed in the following.

4.2 Polyol Synthesis

In the “polyol approach”, the particles are prepared in alkaline ethylene glycol.[54, 65] The advantage of this approach is that no strongly binding stabilization agents are necessary to obtain stable colloids. For this reason the term “unprotected” was established for this system.[54]

In this work a slightly modified synthesis route for Pt NPs was used for all particles. The metal precursor H_2PtCl_6 was reduced upon heating in basic ethylene glycol to form Pt atoms which nucleate and grow to “unprotected” NPs that are 1.2 nm in size.

4.3 Surface Chemistry of “Unprotected” Pt NPs

(Relevant paper: III)

The term “unprotected” NP was introduced because no additional strongly binding stabilizers are necessary to obtain stable colloids.[54] However, the surface of the particles has to be covered by some species. Otherwise they would sinter and

precipitate. This stabilization has been under debate for almost 15 years, but no spectroscopic studies were carried out to unveil the surface chemistry of “unprotected” NPs. A fundamental knowledge about the surface chemistry is, however, required to develop the synthesis of these unique particles and to achieve a deeper understanding for their functionalization (see Fig. 7).

The particles are prepared in alkaline EG.[66] The oxidation of EG provides the electrons for the reduction of the precursor. So far the stabilization has been attributed to OH^- and EG as well as oxidation product of EG (glycolate and acetate, see Fig. 9 reaction pathway 1).[54, 67-68]

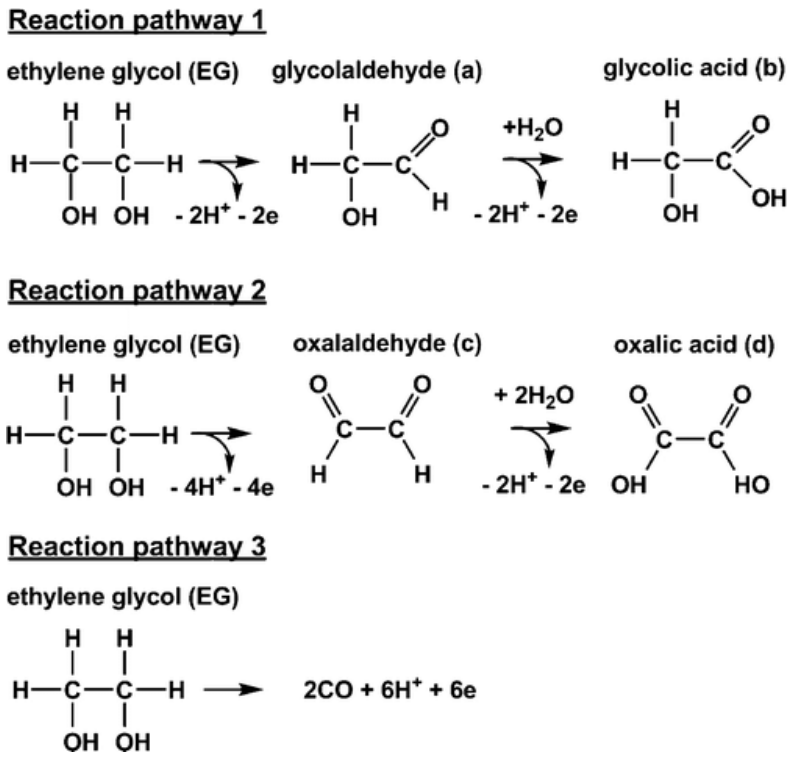

*Figure 9: Reaction pathways for the oxidation of ethylene glycol (EG). “Reprinted with permission from The Journal of Physical Chemistry C, **2015**, 119, 17655-17661. Copyright 2015 American Chemical Society.”*

ESI-MS analysis of the reaction medium after the formation of NPs revealed the presence of glycolaldehyde (a in Figure 9) and glycolic acid (b), oxidation products formed from EG via reaction pathway 1. Also oxalaldehyde (c) from reaction pathway 2 was found. The further oxidation product of this pathway oxalic acids (d) was, however, not found. Oxalic acid readily decomposes to CO_2 under alkaline reaction conditions and can hence be excluded as a stabilizing species.[67] Acetate is not formed within any of the EG oxidation pathways. Indeed acetate was not identified by ESI-MS analysis and can thus be excluded as a stabilizing species.

“Unprotected” Pt NPs were investigated by means of NMR spectroscopy to explore the presence of C-H species on the particle surface (see Fig. 10).

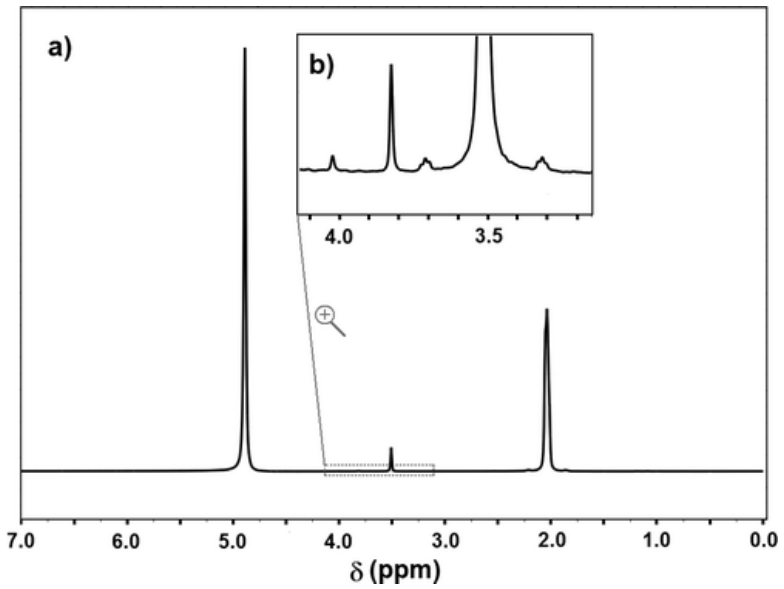

*Figure 10: ^{1}H NMR spectra (360 MHz, 8.4 T, acetone-d_6) of “unprotected” Pt NPs (a) and a zoom from the range 3.2-4.1 ppm (b). “Reprinted with permission from The Journal of Physical Chemistry C, **2015**, 119, 17655-17661. Copyright 2015 American Chemical Society.”*

To measure surface bound species by NMR spectroscopy, the C-H species have to rotate on the surface or exhibit internal rotational degrees of freedom.[69] The latter requirement is fulfilled by all suitable stabilizing species identified from ESI-MS measurements. Thus, these species are expected to be detectable by NMR spectroscopy when being bound to the particle surface. The spectrum (Figure 10a) shows two signals at 3.5 and 4.9 ppm that are attributed to the CH_2 and OH group of EG, respectively. A zoom into the spectrum (Figure 10b) shows two additional signals at 3.8 and 4.0 ppm. The first signal was identified as an organic impurity in the deuterated solvent. The second one could be assigned to glycolic acid, which was also identified by ESI-MS analysis of the reaction medium.

To discriminate if the signals are attributed to free or surface bound species, EG and glycolic acid were added to the sample. The metal core causes a downfield shift of the proton signals in comparison to the free solvated molecule (knight shift).[69-70] The addition of free EG and glycolic acid led to an increase of the present signals, but no additional signals appeared. This test demonstrates that EG and glycolic acid identified by NMR are not bound to the surface, but only dissolved residues that originate from the reaction medium are present and could not be removed completely by sample

rinsing. This correlates with previous studies that report the binding energy of carboxylic ligands on Pt to be too low to bind effectively to Pt surfaces.[71] The NMR investigation clearly reveals that no C-H containing species act as surface bound stabilizers. However, the actual identity of the surface species remained unclear.

Next, the particles were investigated by ATR-IR spectroscopy (see Fig. 11). It has to be considered that NP samples contain unpredictable water residues. Therefore, a spectrum of water in EG (blue spectrum) was recorded, scaled appropriately, and subtracted from the ATR-IR spectrum of the sample (black spectrum) to obtain a spectrum that only reflects features arising from Pt nanoparticles (red spectrum). This spectrum shows one main signal at 2026 cm^{-1}, which could be assigned to linearly adsorbed CO on Pt.[72] Two additional weak signals at around 1730 and 1830 cm^{-1} were attributed to glycolate residues dissolved in the medium and bridge bound CO on Pt, respectively.[73]

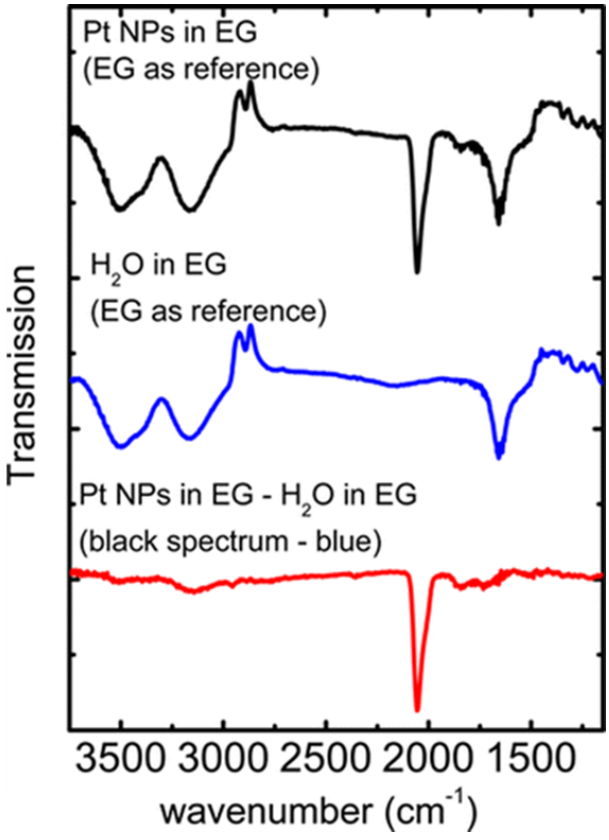

*Figure 11: ATR-IR spectra of "unprotected" Pt NPs in EG (black) and H_2O in EG (blue). The water spectrum was substracted from the Pt NP spectrum to take account for water residues in the sample (red). "Reprinted with permission from The Journal of Physical Chemistry C, **2015**, 119, 17655-17661. Copyright 2015 American Chemical Society."*

The CO can be formed during oxidation of EG (pathway 3 – Figure 9).[74-75] The CO band for as-prepared Pt NPs investigated in this study appeared at 2026 cm^{-1}. While the position of the linear CO band of a fully covered Pt NP surface was around 2060 cm^{-1}.[73] An explanation for this shift can be given by the dependency of the CO on Pt band on its vicinity. On a fully CO saturated surface, adjacent CO molecules vibrate at the same frequency, which causes coupling between neighboring dipoles and a blue-shift of the CO band.[76] A second competing adsorbate on the surface dilutes the number of adjacent CO molecules. This reduces the dipole coupling and results in a shift to lower wavenumbers. In addition, a shift can be induced, because a second competitive adsorbate can alter the electronic properties of Pt and thereby the π-back-donation strength of the metal to CO. The singleton frequency for an isolated CO molecule on the here discussed Pt NPs has been previously determined to be around 2017 cm^{-1}.[73] The position of the CO-stretching mode in the spectrum with respect to the singleton frequency and the signal of a fully covered surface hence indicate the presence of a second species on the surface that dilutes partly the adsorbed CO. From the above mentioned candidates, only OH^- remains as a second potential surface binding species. Due to the water residues in the sample OH^- can neither be determined nor excluded by NMR and IR spectroscopy. For this reason, it was tried to gain evidence for the presence or absence of OH^- via a synthetic approach. When OH^- plays an important role, the stability of the formed colloids should depend on the OH^- concentration. With regard to this idea, different starting concentrations of NaOH were applied and the resulting particle stability was probed.

*Table 2: Starting NaOH concentration for the formation of Pt colloids from 0.01 M H_2PtCl_6 precursor, the corresponding final OH to $Pt_{surface\ atom}$ ratio and the position of the CO band after synthesis. "Reprinted with permission from The Journal of Physical Chemistry C, **2015**, 119, 17655-17661. Copyright 2015 American Chemical Society."*

starting NaOH concentration (M)	**final ratio of $OH^-/Pt_{surface\ atoms}$**	**CO band position (cm^{-1})**
0.500	44.5	2020
0.250	19.1	2026
0.125	6.4	2031
0.094	3.3	2037
0.078	1.7	2042
0.063	0.1	2046

Stable colloids using an H_2PtCl_6 precursor concentration of 0.01 M could only be formed with NaOH starting concentrations between 0.500 and 0.063 M (see Tab. 2). At lower concentrations the particles were not stable but precipitated. The final $OH^-/Pt_{surface\ atoms}$ ratio (here the protons formed during reduction were taken into account) revealed that at lower concentrations the OH^- is completely neutralized after reaction.

This finding indicates that "unprotected" Pt NPs are stabilized by a mixture of CO and OH^-. Changing the amount of OH^- and thus the CO/OH^- ratio during reaction should change the surface coverage of both species. The OH^- coverage has to increase with increasing OH^- starting concentration. This effect can be shown by probing the position of the CO band of the different samples (Table 2). It was found that the CO band shifts from 2020 cm^{-1} for the highest to 2046 cm^{-1} for the lowest NaOH starting concentration. The position of the band reveals that at every tested concentration the surface is covered by CO and OH^-. The CO concentration on the surface, however, increases by decreasing OH^- concentration in the reaction solution. The highest coverage at a NaOH starting concentration of 0.063 M is still 14 cm^{-1} below the value of a fully covered CO surface (2060 cm^{-1}).[73] This indicates that OH^- is essential for the stabilization of the particles under synthesis conditions. Furthermore, the NaOH concentration is expected to effect the particle size as determined by SAXS (see Fig. 12).

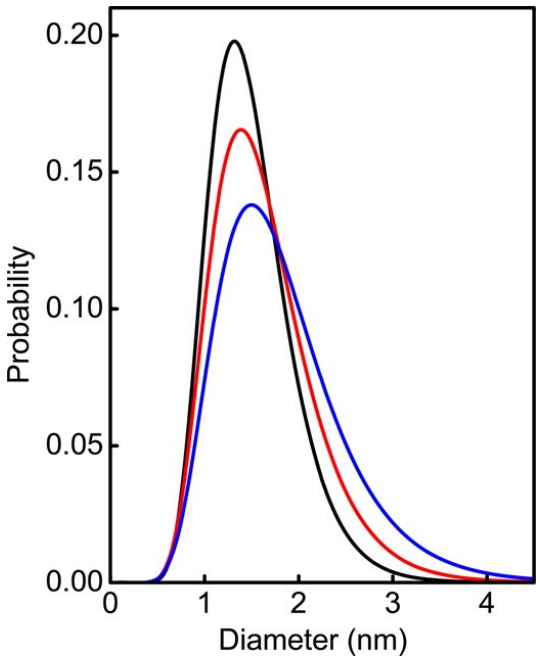

*Figure 12: Particle size distribution for „unprotected" Pt NPs with a starting NaOH concentration of 0.250 M (black), 0.094 M (red), and 0.078 M (blue) determined by SAXS measurements. With decreasing NaOH concentration the distribution broadens and the maximum shifts to larger particles. "Reprinted with permission from The Journal of Physical Chemistry C, **2015**, 119, 17655-17661. Copyright 2015 American Chemical Society."*

When the OH^- concentration is lowered (starting concentration black > red > blue) the particle size increases and the size distribution broadens. This can be explained by the result that OH^- acts as the second protection species. By lowering its concentration the efficiency for protecting the particle decreases, especial for small particles and as a consequence the probability to grow increases. This allows a moderate control over the particle size.

The investigations demonstrate that “unprotected” particles are not free of adsorbates. They are stabilized by CO and OH^-. The presence of OH^- is essential to obtain stable colloids. In order to account for this new knowledge about the stabilization of “unprotected” NPs they will be referred to as "surfactant-free"Pt NPs in future works.[77]

The knowledge about the surface chemistry provides new possibilities for improving their preparation. A decrease of the starting OH^- concentration was found to lead to a moderate increase of the particle size. Recent results demonstrate the possibility to increase the size even further up to 6 nm.[77] This allows for investigating particle size effects in heterogeneous catalysis without the need for surfactant-based syntheses. Furthermore, the influence of the particle size on the catalytic properties of ligand-functionalized NPs becomes determinable.

5. Synthesis and Characterization of Ligand-functionalized Pt NPs

5.1 Choice of Suitable Ligands for Ligand-functionalized Pt NPs

Ligand-functionalized NPs can be prepared with the method described in Section 2 (see Fig. 7). As mentioned above the ligands should bind and remain on the Pt surface during catalysis to act truly as a ligand and obtain a heterogeneous catalyst. An essential requirement for this task is that the ligands are not soluble in the reaction medium. To meet this criterion the ligands have to be hydrophilic (see Section 2), when converting organic reactants in a nonpolar organic solvent. In addition, the ligands have to be enantiopure to achieve a steroselective control. This allows the use of amino acids and their derivatives that exhibit a broad variety of different functional groups such as amino, carboxyl, thiol, thioether, and hydroxyl.

Carboxylic and hydroxyl groups are not suitable as binding groups. The binding of those functional groups to catalytically relevant metal surfaces, like Ru and Pt, is not

effective.[71, 78] Sulfur-based and amino groups, however, can bind to these metal surfaces.[79] So far, most selectivity studies in heterogeneous catalysis utilize thiol ligands.[51, 73, 80-81] The binding energy of thiols to Pt is around 200 kJ·mol^{-1}.[82] Such a strong binding is beneficial for preparation of stable materials, but thiol-stabilized NPs show a decrease in catalytically activity.[80] The reason for this inhibition is twofold i) surface atoms are blocked by binding ligands, ii) the ligands change the electronic properties of the metal. The latter affects activation energies and leads to strong poisoning of the metal surface. In contrast the binding energy of amines is around 100 kJ·mol^{-1}.[83] Amine ligands can also block surface atoms, but they do not alter significantly the electronic properties of the metals.[57]

Both groups seem at first sight suitable as anchoring groups. Thiol groups show a strong binding to late transition metal surfaces. For the here discussed purpose to use ligands as a selectivity controlling element, a strong binding is desired to obtain a high stability of the ligand layer. However, the strong poisoning effect of thiols on e.g. Pt and Ru makes them unsuitable. Cysteine, N-acetyl-cysteine and glutathione with thiol groups as the binding moiety were tested as ligands in the hydrogenation of 2-butanone.[51] It could be shown that the activity compared to “ligand-free” Pt NPs decreases by almost three orders of magnitude, due to the binding of thiol groups. In contrast, amines do not change strongly the surface properties,[57, 79] but their stability is limited. The ligand choice is thus a trade-off between activity and stability. Nevertheless, due to the strong activity inhibition of thiols, the presented studies focused on amines as binding moiety.

In addition to the binding moiety, the ligand should contain further bulky groups or a cyclic structure to reduce its conformational flexibility, because rigid structures are known from homogeneous catalysis to be particularly effective for achieving high stereoselectivities.[19]

5.2 Functionalization of Pt NPs with PRO

(Relevant paper: II)

The first investigations focused on proline (PRO) as a hydrophilic amine ligand for the functionalization of Pt NPs.[84] The rigid ligand structure leads to strongly limited

flexibility. Furthermore, the nitrogen atom in the ring increases the barrier for interconversion.[85]

The preparation of ligand-functionalized particles followed the strategy described above (Section 2). For the characterization of PRO-Pt NPs and to demonstrate the binding, the material was investigated using NMR-spectroscopy and the resulting spectrum was compared to free PRO (see Fig. 13). For the experiments, the PRO-Pt NPs were washed a few times with D_2O and then redispersed in alkaline D_2O. Sample rinsing was performed to remove water residues, which disturb the NMR analysis by a broad H_2O signal.

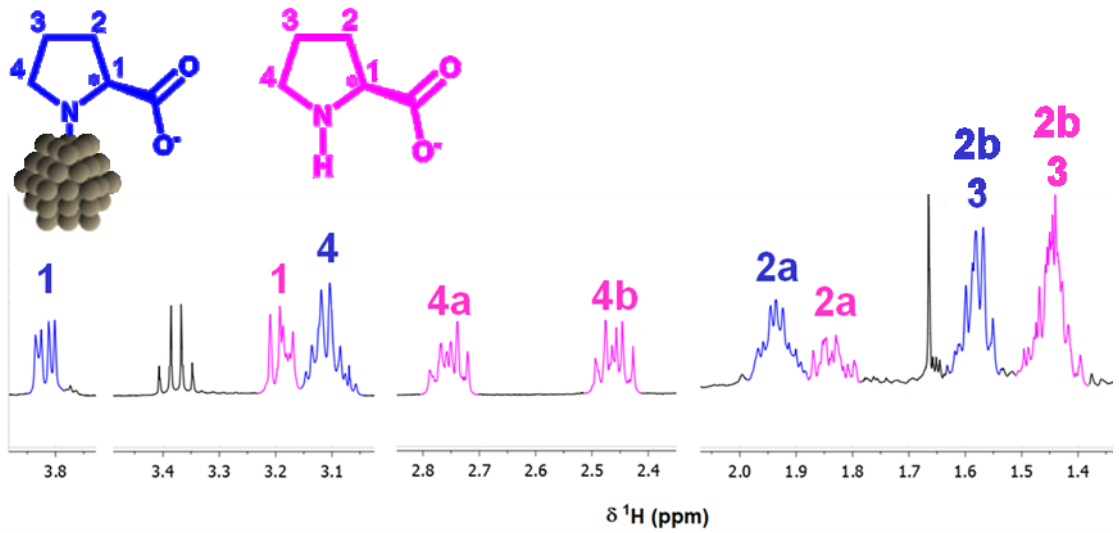

*Figure 13: ^{1}H NMR spectrum (360 MHz, 8.4 T, D_2O) of Pt bound PRO (blue) and unbound PRO (magenta). The black signals are attributed to contaminations. "Reprinted with permission from Journal of the American Chemical Society, **2015**, 137, 905-912. Copyright 2014 American Chemical Society."*

In the recorded NMR spectrum one set of signals (blue one in Fig. 13) and contaminations (black signals) appeared. The organic residues could be identified as ethanol, which was used to remove residual non-binding ligands after functionalization and acetic acid, which is an oxidation product of ethanol. The blue signals could be assigned to PRO.[86] In order to investigate whether this PRO signal pattern is related to free or surface bound PRO, a small amount of free PRO was added to the particle dispersion. This led to the appearance of a second but shifted set of signals (magenta) in the NMR spectrum. The shift of signal in the sample, however, shows that PRO is indeed bound to the surface. The amino group in PRO seems to be the only possible binding moiety. However, to confirm a binding via the amino group the signals of bound and free PRO have to be compared. Signals 1 and 4, which could be assigned to the

carbon groups beside nitrogen (for assignment see PRO structure in Fig. 13) show a larger shift than signals 2 and 3. This shift may be related to the closer approximation to the metal surface or to the amine that is chemically altered via binding to the metal surface.[69-70] This result shows that amine ligands are effectively bound to the surface and are, therefore, suitable for the use as ligand-functionalized catalysts.

In order to show that the binding of ligands does not alter the particle size "ligand-free" Pt NPs were prepared and functionalized with PRO. From both, the "ligand-free" and the PRO-functionalized samples TEM images were taken and the particle size was analyzed (see Fig. 14).

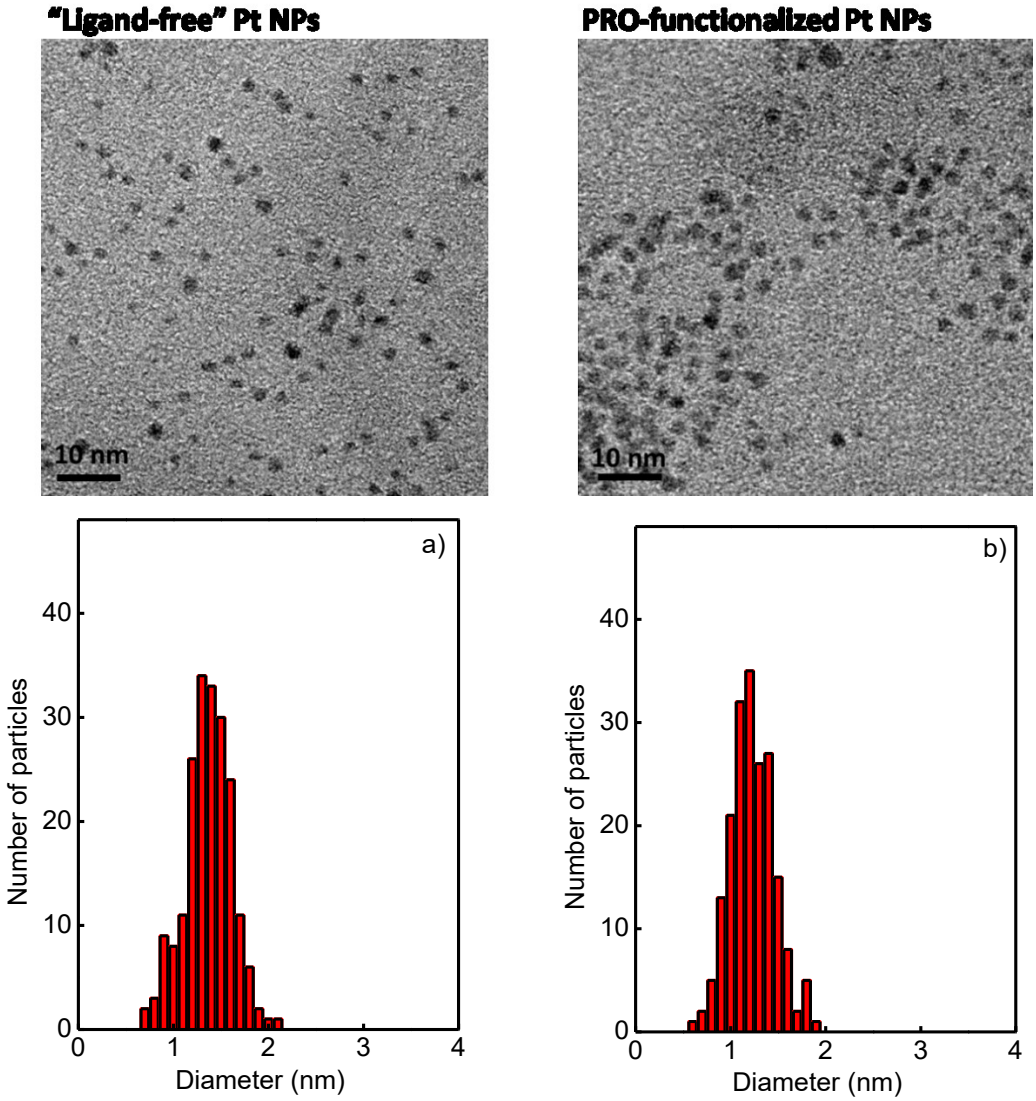

*Figure 14: TEM images (top of Figure) and particle size distributions (lower part) of "ligand-free" Pt NPs (a) and PRO-Pt NPs prepared from this "ligand-free" Pt NPs batch (b). For particle size distribution respectively 200 particles were measured. The particle size distributions don´t show a change in particle size between those samples. A particle size around 1.2 ± 0.3 nm is received. "Reprinted with permission from Journal of the American Chemical Society, **2015**, 137, 905-912. Copyright 2014 American Chemical Society."*

The TEM images and particle size distribution reveal that the binding does not alter the particle size.

In order to determine the ligand coverage,[51] atomic absorption spectroscopy (AAS) and elemental analysis (EA) were performed, which allows determination of the ratio of metal to organic material content. In addition, the ratio of surface atoms to total atoms within the particle (dispersion) is needed. For determination of the dispersion, an fcc packing within the particle was assumed as well as a spherical shape. By taking the particle size of 1.2 nm from TEM measurements into account and a Pt radius of 0.136 nm a particle size of 63 Pt atoms and a dispersion of around 96% was obtained. Using the ratio of metal to organic material content and the dispersion a ligand coverage of 85% was determined.

6. Heterogeneous Catalysis: Hydrogenation Experiments with Ligand-functionalized Pt NPs

In order to perform heterogeneous catalytic investigations, the “unprotected” and ligand-functionalized Pt NPs were deposited onto γ-Al_2O_3 to give nominal metal loadings of 2 wt% Pt. The actual metal loading of every supported catalysts was verified by AAS and used for normalization of the reaction rates.

The hydrogenation experiments were performed in stainless steel autoclaves at a pressure of 20 bar H_2 and at ambient temperature. Conversion and ee of the catalytic experiments were analyzed using a gas chromatograph (GC) equipped with a flame ionization detector (FID). The activity and selectivity of the reaction products were determined from the total amount of detected product and reactant, and by taking the corresponding response factors into account.[87-88] In addition, the carbon balance was tested by using an internal standard, and no significant losses were obtained.

A representative chromatograph of two enantiomeric products for the ee-determination is shown in Figure 15.

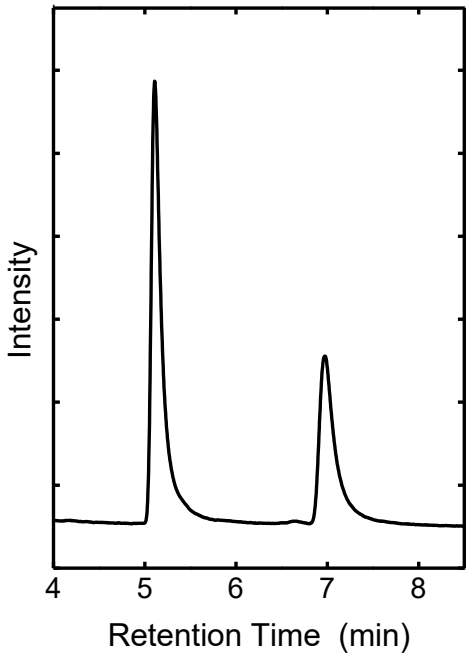

Figure 15: Representative chromatogram for the separation of the two product enantiomers of ethylacetoacetate (tr=5,131 min and 6.995 min, see Fig. 21 for structures). [98] – Reproduced by permission of The Royal Society of Chemistry.

A measure for the stereoselectivity is the ee that is determined by the following equation:

$$ee(\%) = \frac{|m_1 - m_2|}{m_1 + m_2}$$

For reaction rate measurements the conversion was kept below 10% to achieve differential operation conditions.[89] The reaction rates in this thesis are given as turnover frequency (TOF):

$$TOF\left(\frac{1}{h}\right) = \frac{dn_P}{dt} \cdot \frac{M(Pt)}{m(Pt) \cdot dispersion}$$

6.1 Simultaneous Enhancements of Catalytic Activity and Selectivity of Pt NPs induced by PRO

(Relevant paper: II)

Supported N-methyl-PRO and PRO-functionalized Pt NPs were applied as heterogeneous catalysts for the hydrogenation of acetophenone (see Fig. 16).[84] This reactant represents a chemoselective challenge for heterogeneous catalysts. Besides

the desired hydrogenation of the carbonyl group, also the hydrogenation of the aromatic ring can occur. The reaction is, furthermore, a stereoselective challenge, because during the formation of the desired alcohol a stereogenic center is generated.

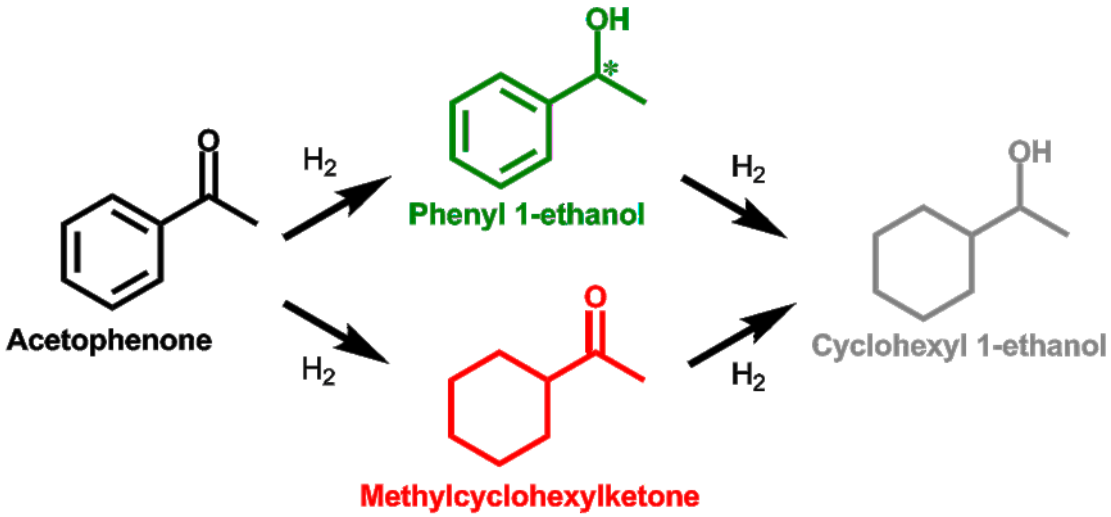

*Figure 16: Hydrogenation of acetophenone (black). The desired reaction is the chemoselective hydrogenation of the carbonyl group (green). Besides this, also the aromatic moiety can be hydrogenated (red) .Both products can further hydrogenated to the fully hydrogenated product (grey). During the desired hydrogenation of the C=O a stereogenic center is formed as indicated with * in green structure. "Reprinted with permission from Journal of the American Chemical Society, **2015**, 137, 905-912. Copyright 2014 American Chemical Society."*

The hydrogenation experiments were first performed with "ligand-free" Pt NPs supported on γ-Al_2O_3 in order to obtain a benchmark for investigating the effect of ligands (see Fig. 17 on the left). The color code reflects the products shown in Figure 16. As only surface atoms are able to contribute to the catalytic reaction, the formation rates were normalized to the total number of surface atoms.

Over "ligand-free" Pt NPs mainly the hydrogenation to the desired unsaturated alcohol (green) occurs, but also significant amounts of undesired side products are formed. This demonstrates the limitations of supported Pt NPs for chemoselective hydrogenations of carbonyl compounds.[31]

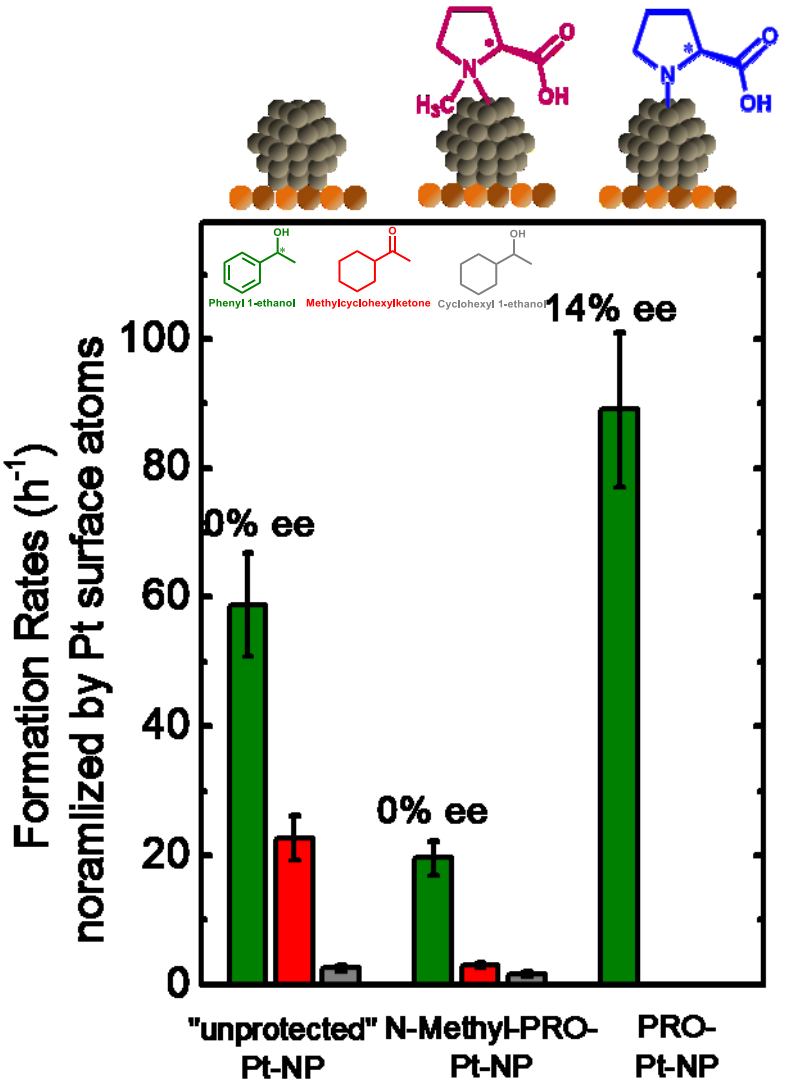

Figure 17: Formation rates normalized to the total number of Pt surface atoms for the hydrogenation of acetophenone over "ligand-free", N-methyl-PRO-Pt and PRO-Pt NPs. The color code reflects the products shown in Figure 16 and in the diagram. The hydrogenation with "ligand-free" and N-Methyl-PRO-Pt NPs form a significant amount of side products. Only the hydrogenation with PRO-Pt NPs proceed 100% chemoeselective. Enantioselectivities (see values on top of columns) could only obtained with PRO. The experimental error for the ee is ±1%. All experiments were performed in autoclaves with 1 mL acetophenone, 9 mL cyclohexane, and 200 mg catalyst. The reaction pressure was 20 bar H_2, the reaction temperature 293 K, and the stirring speed 800 rpm. The conversion was kept below 10%. "Reprinted with permission from Journal of the American Chemical Society, ***2015****, 137, 905-912. Copyright 2014 American Chemical Society."*

When Pt NPs were functionalized with N-methyl-PRO (see Fig. 17), the activity was reduced, but not as strong as compared to the use of thiols,[80] which demonstrates the advantage of using amine based ligands over thiols. The chemoselectivity towards the desired product was increased when N-methyl-PRO was used as a ligand, but still significant amounts of side products were obtained.

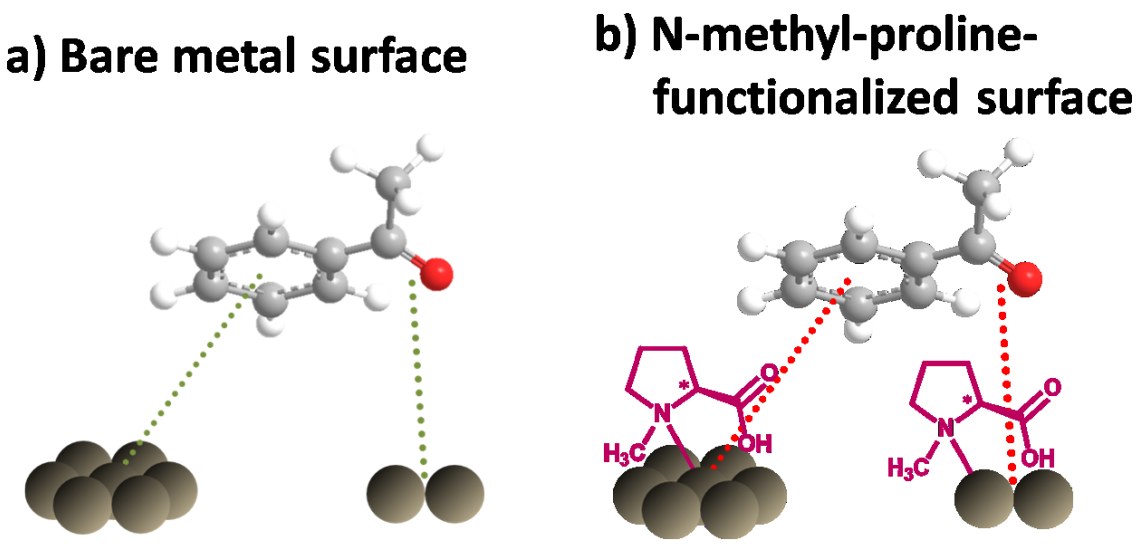

Figure 18: The ensemble effect describes the different number of adjacent surface atoms that are necessary to adsorb and activate different functional groups. Here, as illustrated in the scheme, the aromatic moiety needs a larger ensemble than the C=O group (a). Surface atoms to which a ligand is bound are assumed to be blocked. Ligands thus block ensembles of adjacent surface atoms and hinder the adsorption and hydration of the reactant (b).

The enhanced chemoselectivity at the expense of activity can be explained by the so-called ensemble effect known from bimetallic heterogeneous catalysis (see Fig. 18).[90-92] Different functional groups require different ensembles of adjacent surface atoms for adsorption and activation on metal surfaces. For the hydrogenation of the aromatic moiety larger ensembles of adjacent surface atoms are necessary than for the hydrogenation of the carbonyl group (see Fig. 18a).[90-91, 93] Surface atoms that bind ligands are assumed to be blocked and not to be able to contribute to the catalytic reaction. The binding of ligands and thus the blocking of surface atoms decreases the size of ensembles of adjacent surface atoms. As a result, the number of large ensembles decreases more strongly than the number of small ensembles. This favors the hydrogenation of the carbonyl group leading to an enhanced chemoselectivity at the expense of activity, an effect known form bimetallic heterogeneous catalysis.[94] The ligand coverage of N-methyl-PRO is only 0.4. To improve the chemoselectivity further, presumably higher ligand coverages are necessary, to achieve complete dilution of all large ensembles.

The lower steric demand of PRO in comparison to N-mehtyl-PRO leads to a ligand coverage of 0.85. Hydrogenation experiments performed with PRO-Pt NPs result in a 100% chemoselective conversion to the desired alcohol. The chemoselectivity is, however, not accompanied by a loss of activity. Instead an enhanced rate compared

to “ligand-free” Pt NPs is observed. To discuss the formation rates of “ligand-free” and functionalized particles representatively, it has to be considered that only ligand-free surface atoms are expected to contribute to the reaction. To take this into account the rates were normalized to the number of ligand-free surface atoms (see Fig. 19).

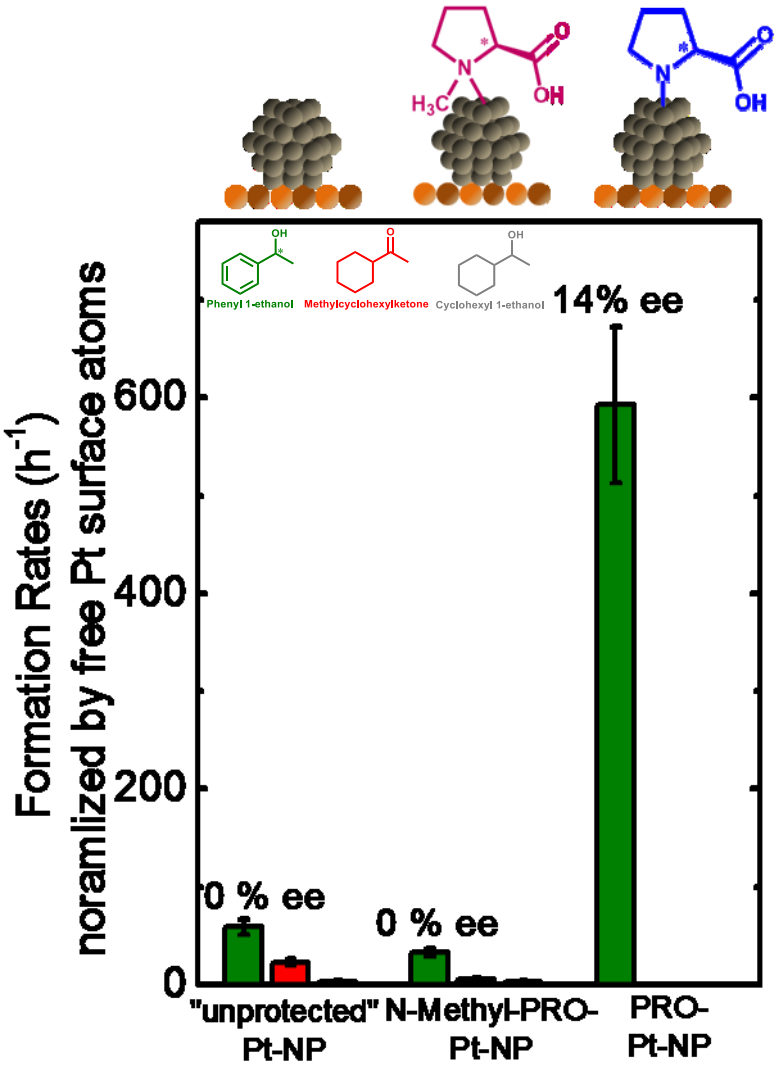

*Figure 19: Formation rates for the hydrogenation of acetophenone over “ligand-free”, N-methyl-PRO- and PRO-Pt NPs shown in Figure 17 normalized to the number of free Pt surface atoms. The color code reflects the products shown in Figure 16 and in the diagram. The hydrogenation with N-Methyl-PRO-Pt proceeds with a slightly decrease in activity and a slightly increase in chemoselectivity compared to “ligand-free” Pt NPs, while the hydrogenation with PRO-Pt NPs shows a significant rate enhancement with 100% chemoselectivity. Values on top of the columns show the enantioselectivity. The experimental error for the ee is ±1%. All experiments were performed in autoclaves with 1 mL acetophenone, 9 mL cyclohexane, and 200 mg catalyst. The reaction pressure was 20 bar H_2, the reaction temperature 293 K, and the stirring speed 800 rpm. The conversion was kept below 10%. “Reprinted with permission from Journal of the American Chemical Society, **2015**, 137, 905-912. Copyright 2014 American Chemical Society.”*

The rates for N-methyl-PRO-Pt NPs still show a slight decrease in activity in comparison to "ligand-free" Pt NPs, while PRO-Pt NPs show a pronounced rate enhancement. As described above, ligands can dilute large ensembles in favor to small

ones. However, this effect that is known from bimetallic heterogeneous catalysis cannot explain the 18 times higher activity of PRO-Pt NPs compared to “ligand-free” Pt NPs. Instead a model from homogeneous catalysis must be applied, the so-called “N-H effect” originally proposed by Noyori et al (see Fig. 20). [95-96]

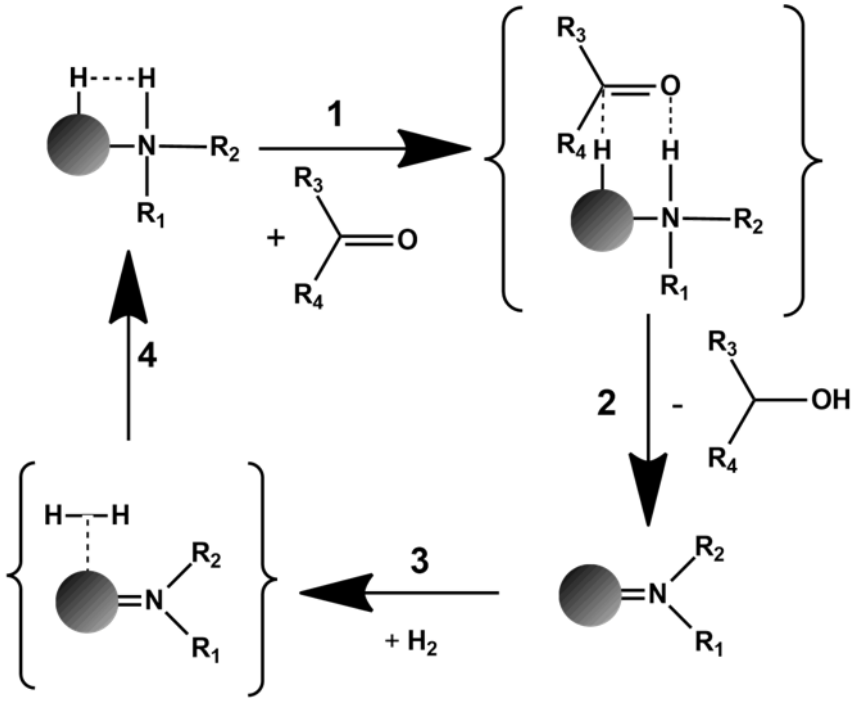

*Figure 20: The “N-H effect” leads to a ligand-accelerated hydrogenation of carbonyls proposed by Noyori et al. The amine bound hydrogen becomes acidic upon binding to the Pt NP and interacts with the carbonyl oxygen of the reactant. This activates the reactant (1). The oxygen is protonated by the amine hydrogen while a hydride is transferred from the metal surface to the carbon atom (2). Then the catalytic species is reformed by adsorption of molecular hydrogen (3) and heterolytic dissociation of this molecular hydrogen (4). “Reprinted with permission from Journal of the American Chemical Society, **2015**, 137, 905-912. Copyright 2014 American Chemical Society.”*

It is known that amine bound hydrogen substituents become acidic upon binding to a late transition D-metal like Pt.[95, 97] These acidic amine protons interact with the carbonyl oxygen of the reactant, leading to an enhanced activation of the reactant (step 1 in Figure 20). The hydrogenated product is formed, due to protonation of the oxygen by the amine hydrogen and hydride transfer from the metal surface to the carbon atom (step 2 in Figure 20). By adsorbing molecular hydrogen (step 3 in Figure 20) and subsequent heterolytic dissociation the catalytic species is reformed (step 4 in Figure 20). This mechanisms leads to an alternative reaction pathway, which proceeds with an enhanced rate compared to the purely metal catalyzed reaction. Combining this model with the ensemble effect allows to explain the high chemoselectivity and enhanced activity. First, ensembles are diluted by blocking of adjacent surface atoms. Second, the activity of the remaining ligand-free surface atoms is enhanced by the “N-

H effect".[96] In contrast, a tertiary amine (N-methyl-PRO) does not have an N-bound hydrogen substituent. The ligand-accelerated hydrogenation described in Figure 20 can hence not proceed, but only the purely metal catalyzed reaction pathway. N-methyl-PRO thus acts only as a surface blocking species and the lower ligand coverage explains the lower chemoselectivity compared to PRO-Pt NPs.

In addition to the rate enhancement and the control of chemoselectivity the PRO-Pt NP system showed some modest stereoselectivity (values on top of the columns in Figure 17 and 19). In following sections it will be shown how within the PhD studies the stereoselectivities could be enhanced to more than 70% ee.

6.2 Effect of Particle Size and Ligand Configuration on Catalytic Properties

(Relevant paper: IV)

The mechanistic understanding from homogeneous catalysis was so far used as guidance for the development of the ligand-functionalized Pt NP catalysts. However, homo- and heterogeneous catalysts are distinctively different materials. Metalorganic catalysts consist of a single metal atom surrounded by ligands. In contrast, the surface of a NP is formed from several atoms that differ in terms of geometric and electronic properties and these further change with particle size. As a result, ligands bound to different surface atoms can also be chemically and catalytically different. This may lead to unpredictable effects on the activity and selectivity when changing the particle size.

To explore the effect of particle size a β-ketoester (ethyacetoacetate (EAA)), was used as a test reactant (see Fig. 21), for which high ees can be obtained with homogeneous catalysts.[96, 98]

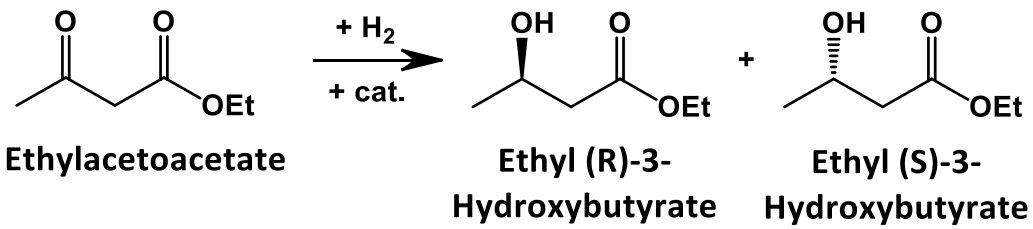

Figure 21: Catalytic hydrogenation of ethylacetoacetate. The reaction proceeds chemoselective to ethyl (R)-3-hydroxybutyrate and ethyl (S)-3-hydroxybutyrate. [98] – Reproduced by permission of The Royal Society of Chemistry.

This reaction was a first step towards higher stereoselectivity. When being hydrogenated with PRO-Pt NPs an ee of 34% was obtained. In contrast to acetophenone (see Fig. 16) EAA does not represent a chemoselective problem, because only the keto group is reactive, while the ester group is unreactive under the applied reaction conditions.[99] As described above (Section 4.3) different particle sizes can be synthesized by varying the OH^- concentration within the particle synthesis.[66] In order to investigate the effect of particle size "ligand-free" and PRO-functionalized particles with a size of 1.2 ± 0.3 and 2.1 ± 0.5 nm were prepared. Both particle sizes are in the mitohedrical region below 5 nm, where the ratio of low to highly coordinated surface atoms changes strongly.[100] The two particle sizes are thus suitable to investigate the relevance of size effects.

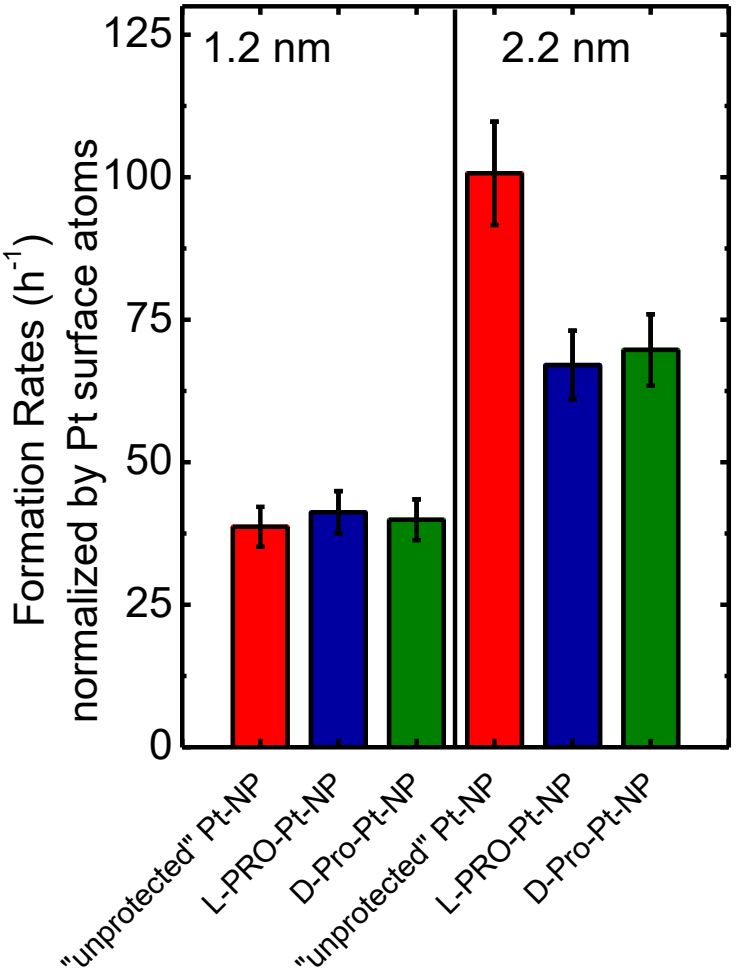

Figure 22: Formation rates for the hydrogenation of ethylacetoacetate normalized to the number of Pt surface atoms. The hydrogenation was performed over "ligand-free" (red), L-PRO-Pt (blue) and D-PRO-Pt NPs (green) with particle sizes of 1.2 nm (left) and 2.1 nm (right). The functionalization with PRO slightly reduces the activity of the larger particles, while the activity for the smaller ones remains constant. Additionally the larger particles are more active than the smaller ones. All experiments were performed in autoclaves with 1 mL ethylacetoacetate, 9 mL THF, and 200 mg catalyst. The reaction pressure was 20 bar H_2, the reaction temperature 298 K, and the stirring speed 800 rpm. The conversion was kept below 10%. [98] – Reproduced by permission of The Royal Society of Chemistry.

The formation rates normalized to the number of Pt surface atoms (see Fig. 22) for the hydrogenation of EAA clearly demonstrate that the particle size alters the activity. The activity (normalized to the number of surface atoms) for “ligand-free” Pt NPs increases by a factor of 2.7 by increasing the particle size from 1.2 to 2.1 nm. For PRO-Pt NPs still a 1.7 fold enhancement is observed. This findings has been previously reported for the hydrogenation of carbonyls over Pt NPs and related to decarbonylation of the reactant by low-coordinated surface atoms.[101] Thus formed CO can strongly bind to such low-coordinated Pt and poison them.[102] To validate this explanation IR spectroscopic measurements were performed before and after exposure of PRO-Pt NPs to reaction conditions (see Fig. 23).

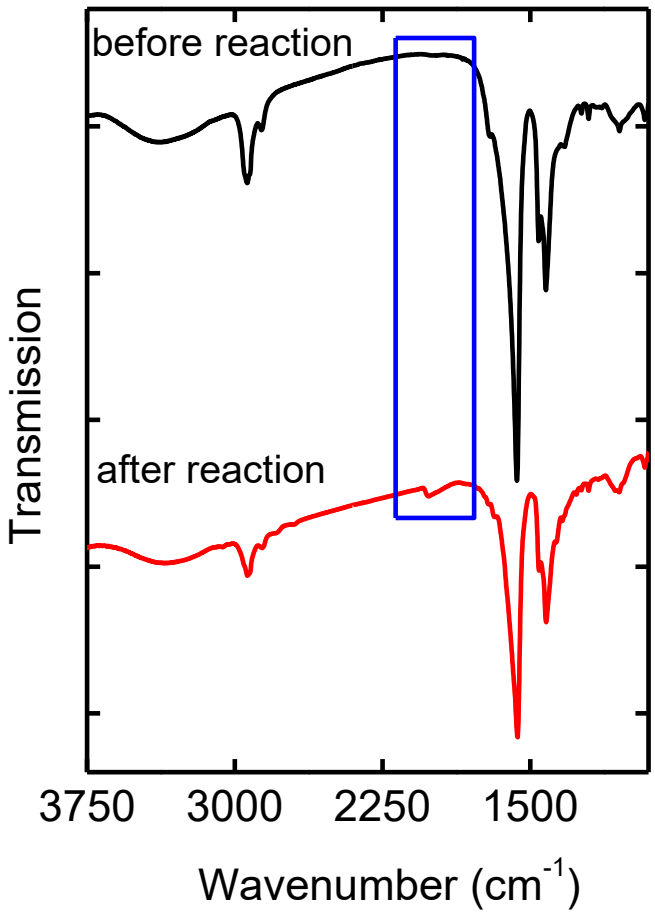

Figure 23: IR spectra of PRO-Pt NPs supported on a SI wafer recorded before (black) and after hydrogenation reaction (red). After hydrogenation reaction a further band at 2016 cm^{-1} is observed that can be related to linear adsorbed CO on Pt. [98] – Reproduced by permission of The Royal Society of Chemistry.

After reaction an additional band appears around 2016 cm^{-1} that is characteristic for the stretching mode of CO adsorbed on Pt.[76] The formation of CO is thus confirmed spectroscopically explaining the obtained effect of the particle size on the catalytic

activity. As described above (Section 4.3) the position of the CO band gives information about the CO coverage. The singleton frequency for adsorbed CO was determined to be 2017 cm^{-1}.[73] It can thus be assumed that the CO is isolated on the surface, which in turn fits with the high ligand coverages determined for PRO (see Tab. 3).

Comparison of "ligand-free" and PRO-functionalized particles shows for the smaller particles nearly the same activity although during functionalization around 80-85% of surface atoms are expected to be blocked by ligands. As described in Section 5.1 an electronic effect by binding amine ligands can be excluded.[57] This underlines that also for EAA the N-H assisted reaction pathway occurs (see Fig. 20), which proceeds with a higher rate than the purely metal-catalyzed reaction.[95-96] In contrast to small particles, on larger particles a decrease in activity is obtained by functionalization with PRO. As described above the binding of ligands to surface atoms reduces the number of surface atoms which participate within the reaction. On larger particles an even higher ligand coverage of 93-96% is obtained (compare Table 3), which can explain the reduced reaction rate.

Table 3: Enantiomeric excess and ligand coverage for the hydrogenation of ethylacetoacetate over ligand-functionalized Pt NPs of different particle size. For functionalization L-PRO and D-PRO were used (see top of table for catalyst structure). With increasing particle size the ligand coverage increases. A positive ee corresponds to an excess in formation of ethyl (R)-3-hydroxybutyrate and a negative ee to an excess of ethyl (S)-3-hydroxybutyrate (see Fig. 21). The change of particle size has no effect of enantioselectivity. Different ligand configurations lead to an enatioselectivity of same magnitude, but with change in product configuration, as indicated by the algebraic sign. All experiments were performed in autoclaves with 1 mL ethylacetoacetate, 9 mL THF, and 200 mg catalyst. The reaction pressure was 20 bar H_2, the reaction temperature 298 K, and the stirring speed 800 rpm. The conversion was kept below 10%. [98] – Reproduced by permission of The Royal Society of Chemistry.

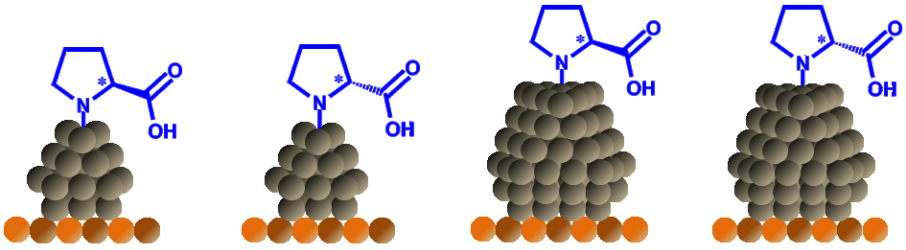

Catalyst	L-PRO-Pt (1.2 nm NPs)	D-PRO-Pt (1.2 nm NPs)	L-PRO-Pt (2.1 nm NPs)	D-PRO-Pt (2.1 nm NPs)
Enantiomeric Excess (%)	34 (± 2)	-30 (± 2)	30 (± 2)	-33 (± 2)
Ligand coverage	0.85	0.8	0.96	0.93

The high coverage of PRO on the Pt NPs (see Tab. 3) diminishes the probability that adjacent bare surface atoms are present, and the remaining ligand-free surface atoms

can be assumed to be isolated, as indicated by the IR spectroscopic findings. A purely metal catalyzed reaction on PRO-Pt NPs can thus been excluded, because hydrogenation reactions are expected to require two adjacent surface atoms. One surface atom is needed for the activation of EAA and an adjacent surface atom for the activation of hydrogen.[103] The above discussed N-H mechanism (see Fig. 20) known from homogeneous catalysis requires only one free adsorption site for the activation of molecular hydrogen. However, in contrast to the labile ligand sphere of a metal-organic compound Pt NPs have a rigid surface and every surface atom exhibits adjacent metal atoms. It seems thus unlikely that only one single surface atom to which a ligand is bound is able to perform the different reaction steps needed for the postulated mechanism. Instead, it is more likely that a bare Pt surface atom is required adjacent to the ligand-binding atom in order to bind and activate hydrogen (see Fig. 24). This in turn means that due to the high ligand coverage of PRO-Pt NPs the reaction is limited by the availability of "ligand-free" surface atoms. In this way the moderate decrease in activity for large particles upon functionalization with PRO can be explained based on the ligand coverage (see Tab. 3), while no effect was found for the small particles.

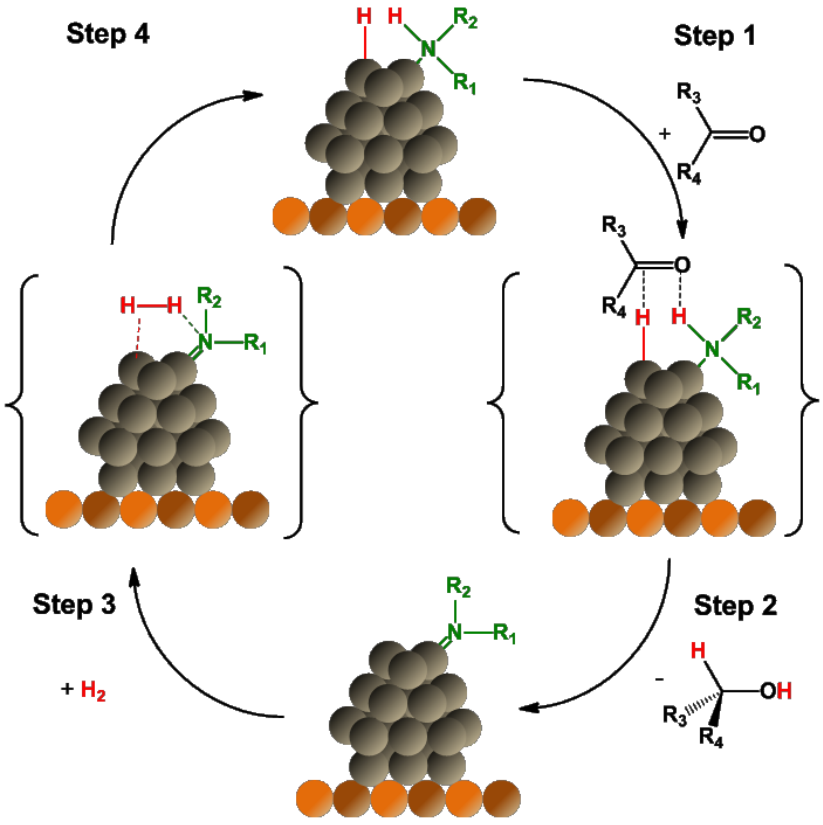

Figure 24. Extended N-H assisted reaction pathway on a "ligand-blocked-ligand-free" pair site. The carbonyl-C of the reactant interacts with the Pt bound hydride and the oxygen with the amine bound hydrogen (step 1). The reactant gets hydrogenated (step 2). Then molecular hydrogen is adsorbed and heterolytically dissociated (step 3), and the reactive species is reformed (step 4). [98] – Reproduced by permission of The Royal Society of Chemistry.

So far only activities have been discussed. The comparison of the enantioselectivities obtained for the two particle sizes reveals that the particle size does not alter the enantioslectivity (see Tab. 3). This can be explained by the proposed extended N-H assisted reaction pathway. It is assumed that the reactant is not in direct contact with the metal surface. Changes in the surface properties do thus not necessarily influence the reaction, and the stereoselectivity is primarily determined by the ligand-reactant interaction, similar as in homogeneous catalysis. In contrast to this finding, the chiral modifier system shows a strong particle size dependence for the enantioselectivity.[104] The ee increases with particle size. In these systems the reactant and modifier have to adsorb in a flat-lying mode on the particle surface, which occurs preferably on large particles with extended surfaces.[105]

A further interesting finding was obtained as the ligand configuration was changed. The absolute ee values are the same irrespective of the ligand configuration, but product configuration is inverted (see Tab. 3). This finding is similar to homogeneous catalysis[106] and the modifier systems[107] where the product configuration can also be controlled by ligand configuration.

Overall, the discussed findings for the stereoselective control suggest that primarily the ligand-reactant interaction determines the stereoselective control. This result is of significant importance, because it shows that ligand-functionalized NPs are less complex than chiral modifiers, where e.g. the particle size has a strong influence. Furthermore, it reveals that the search for systems with enhanced stereoselectivities can be reduced to find ligand-reactant combinations with a perfect fit.

6.3 Optimization of Functionalization for Catalytic Applications

The ligand-reactant interaction has been elucidated as the key for the control of stereoselectivity. A ligand-controlled reaction can, however, only be effective if background reactions, proceeding on the bare metal surface, are suppressed. In Section 6.1 it was discussed that the ligand coverage determines the chemoselectivity. N-methyl PRO-Pt NPs with a ligand coverage of 0.4 lead to a chemoselectivtiy of 81%, while PRO-Pt NPs with a higher ligand coverage of 0.85 are 100% chemoselective.[84] It was concluded that the chemoselectivity increases with ligand coverage and remains constant as a certain ligand coverage is achieved at which all ensembles are diluted

by ligands. A high coverage is necessary to guaranteed 100% chemoselectivity. In Section 6.2 it was described that the ligand coverage determines the activity. Here both investigated ligand coverages were so high that a purely metal-catalyzed reaction pathway was inhibited. A higher coverage led only to a decrease in activity as the number of “ligand-free” surface atoms, needed for H_2 activation, is further reduced.[98] The ligand concentration within the functionalization step is thus an important parameter which determines the ligand coverage and in this way the selectivity. The functionalization of NPs with amino acids proceeds in a basic aqueous solution (NaOH) to ensure deprotonation of the amino group. The free electron pair of the amino group is required to form the metal-ligand bond. However, at high NaOH concentrations within the functionalization, OH^- can act as a ligand and compete with PRO.[108] Thus, besides the ligand concentration, also the OH^- concentration is an essential parameter for the binding of the ligands to the particle. To investigate the influence of the functionalization on the activity and enantioselectivity, hydrogenation experiments were performed with different PRO-Pt NP samples. PRO was chosen due to the best catalytic results so far. As a model reaction the hydrogenation of the simplest β-ketoester, methylacetoacetate (MAA) was used (see Fig. 25).

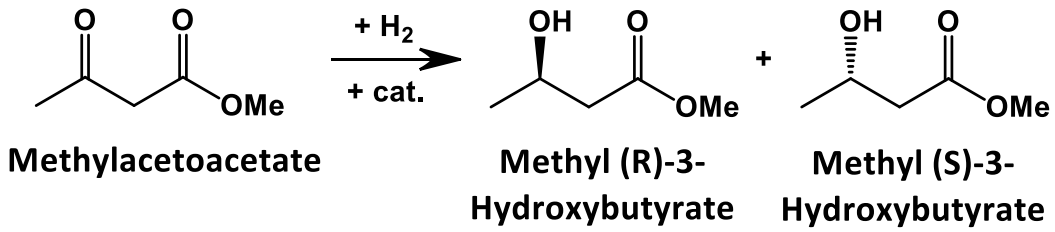

Figure 25: Catalytic hydrogenation of methylacetoacetate. The reaction proceeds chemoselective to methyl (R)-3-hydroxybutyrate and methyl (S)-3-hydroxybutyrate.

In order to determine the optimal ligand to OH^- ratio for the ee, PRO-Pt NPs functionalized with different PRO concentrations and two different NaOH concentrations (25 mM, 30 mM) were investigated for the hydrogenation of MAA (see Fig. 26).

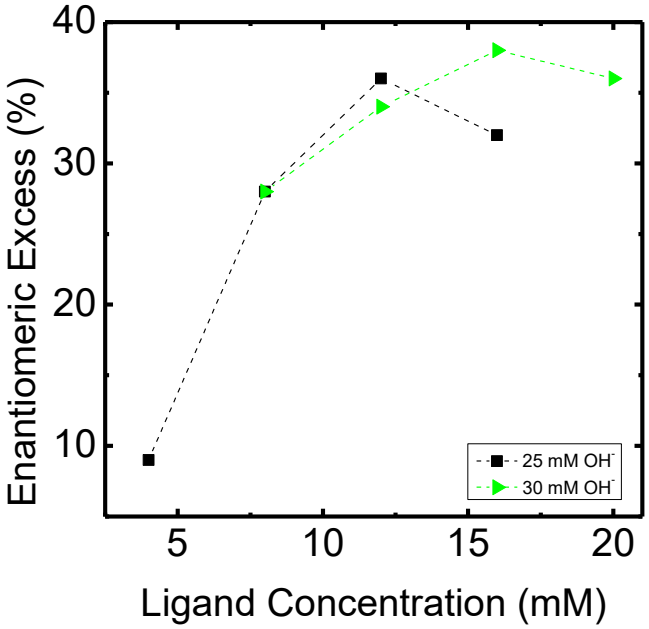

Figure 26: Hydrogenation experiments of methylacetoacetate with different functionalized PRO-Pt NPs. The functionalizations were performed with two fixed OH^- concentration of 25 (black) and 30 (green) mM and different ligand concentrations. The experimental error for the ee is ±1%. All experiments were performed in autoclaves with 1 mL methylacetoacetate, 9 mL THF, and 200 mg catalyst. The reaction pressure was 20 bar H_2, the reaction temperature 298 K, and the stirring speed 800 rpm. The conversion was kept below 10%.

As described above, both concentrations depend on each other. It is not the ligand concentration that determines the ligand coverage, but the concentration of deprotonated ligands and the remaining OH^- ions. For both investigated OH^- concentrations (see Fig. 26) a ligand to OH^- ratio of 0.5 during functionalization was found to give the best ees (~ 38%). Under these conditions the ligands are effectively deprotonated and the OH^- concentration is low enough so that OH^- does not effectively compete with the ligand for binding sites at the particle surface.

In the next step the ligand and the NaOH concentration were both varied, but at constant ratio of 0.5 ligand to NaOH. The resulting effect on the activity and ee is shown in Figure 27.

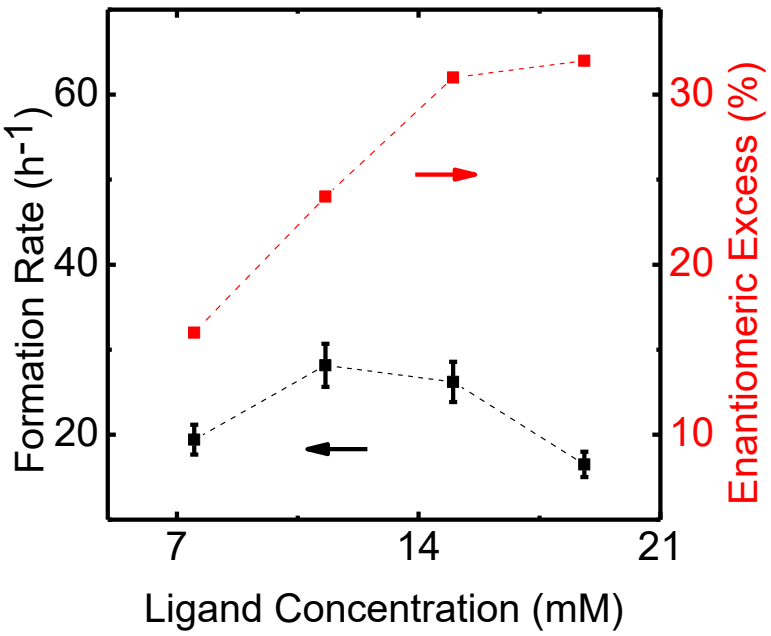

Figure 27: Formation rates normalized to the number of all Pt surface atoms (left axis) and enantioselectivities (right axis) for the hydrogenation of methylacetoacetate. The hydrogenation was performed with different functionalized PRO-Pt NPs. The ligand and the NaOH concentration were simultaneously varied in the functionalization, but at constant ligand to NaOH ratio of 0.5 (best results in Fig. 26) and a fixed metal content in order to get the optimal ligand to metal ratio. The experimental error for the ee is ±1%. All experiments were performed in autoclaves with 1 mL methylacetoacetate, 9 mL THF, and 200 mg catalyst. The reaction pressure was 20 bar H_2, the reaction temperature 298 K, and the stirring speed 800 rpm. The conversion was kept below 10%.

A volcano-like plot was obtained with increasing ligand concentration (constant ratio of 0.5 ligand to NaOH) for the reaction rate. First the reaction rate increases with ligand concentration, as the NH-assisted pathway gets more favored, which proceeds with a higher rate than the purely metal-catalyzed reaction. At a certain ligand coverage the purely metal-catalyzed reaction pathway is completely suppressed and the reaction becomes limited by the availability of “ligand-free” surface atoms, needed to activate hydrogenation (see Fig. 27). As a result the activity decreases as the ligand coverage is further increased. In contrast, the enantioselectivity increases with decreasing probability of the purely metal catalyst reaction pathway and remains constant when this pathway is suppressed. The highest ees were obtained for a ligand concentration of 16 mM and higher. This concentration reflects the optimal preparation conditions to achieve the ligand density required for obtaining the best stereoselective control. From this point on only the activity continues to decrease as the ligand concentration is further increased. The ligand concentration was thus fixed to 16 mM for the following studies.

In addition to the ligand concentration also the OH^- concentration may influence the performance of the catalyst as described above. However, from previous studies it is known that beside the ligand also OH^- can bind to the particle surface and both may compete for binding sites. In order to determine the influence of the OH^- concentration, ligand solutions with the optimized ligand concentration (16 mM) but different NaOH contents were used to prepare differently functionalized PRO-Pt NPs. The resulting effects on the catalytic performance are shown in Figure 28.

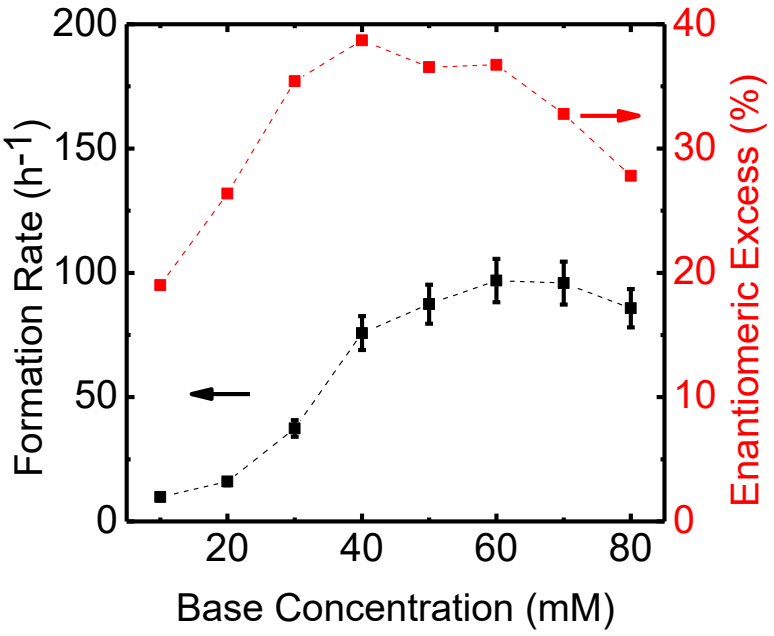

Figure 28: Hydrogenation experiments of methylacetoacetate with different functionalized PRO-Pt NPs. The functionalizations were performed with a fixed ligand concentration of 16 mM and different OH^- concentrations. The experimental error for the ee is ±1%. All experiments were performed in autoclaves with 1 mL methylacetoacetate, 9 mL THF, and 200 mg catalyst. The reaction pressure was 20 bar H_2, the reaction temperature 298 K, and the stirring speed 800 rpm. The conversion was kept below 10%.

The ee, as well as the activity, show a volcano-like dependence on the NaOH concentration. First, the base is necessary to deprotonate the amino group, which enables for an effective binding of the ligand to the surface. This effect is reflected by the increase in activity and selectivity. However, at OH^- concentration of 40 mM and higher the ee decreases. The same trend but slightly shifted to higher NaOH concentrations is obtained for the activity. This shows the starting competition between OH^- and PRO for binding sides leading to a decrease in activity and selectivity.

It could be shown that by optimizing the functionalizing conditions the enantiomeric excess and the activity are enhanced. In fact the ee could be raised from 34% to 39%.

This trend should also hold for other ligands. However, it has to be considered that every ligand has different pKs values for the deprotonation of the amino group (see Fig. 29). The acid-base properties differ and should affect the functionalization with these ligands.

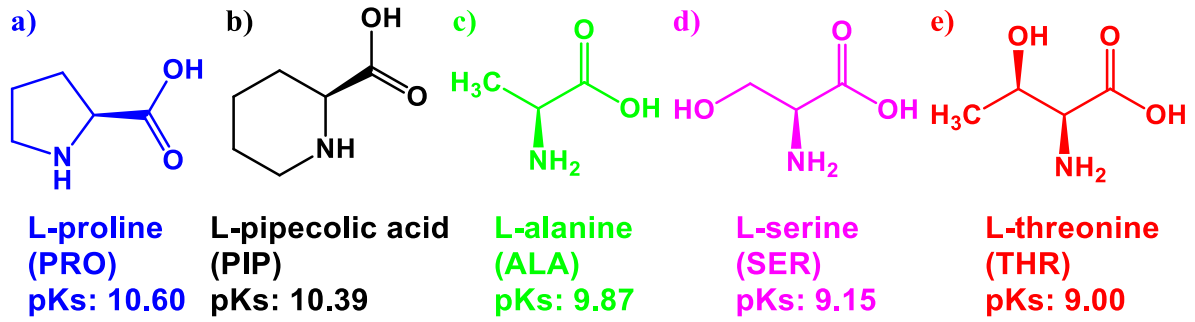

Figure 29: Ligand structures for the investigation of functionalization conditions.

To test for this hypothesis a ligand that differs only in ring size to PRO, thus exhibiting a similar pKs value (see Fig. 29b), and ligands of clearly different pKs values were tested (29c-e). To receive a trend which represent mainly the change in pKs values, ligands with similar structures were chosen.

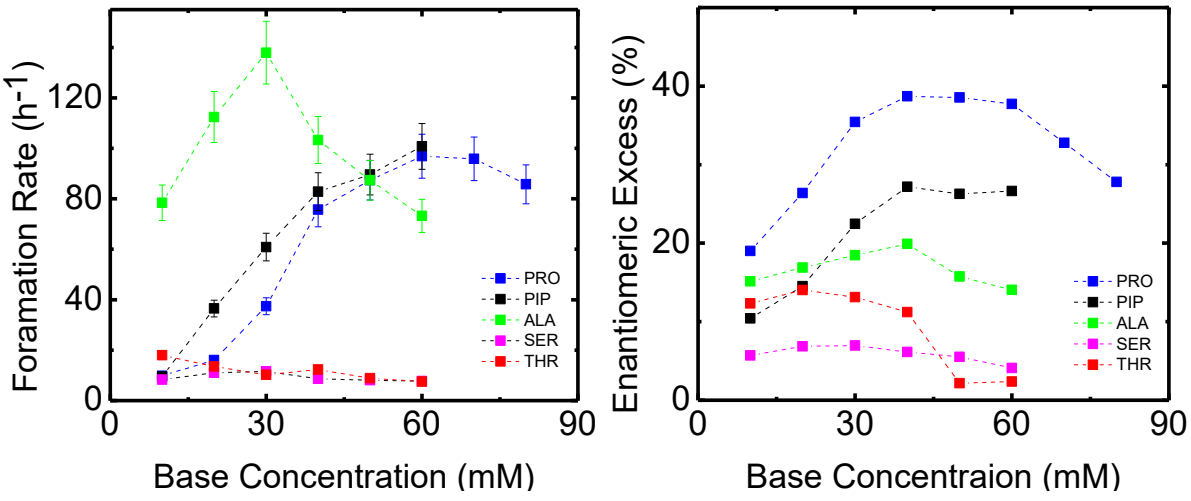

Figure 30: Hydrogenation experiments of methylacetoacetate over different ligand-functionalized Pt NPs. The functionalizations were performed with a fixed ligand concentration of 16 mM and different OH^- concentration. The experimental error for the ee is ±1%. All experiments were performed in autoclaves with 1 mL methylacetoacetate, 9 mL THF, and 200 mg catalyst. The reaction pressure was 20 bar H_2, the reaction temperature 298 K, and the stirring speed 800 rpm. The conversion was kept below 10%.

The results (see Fig. 30) for the different ligands show the same trend as PRO-functionalized Pt NPs. Depending on the pKs constant of the NH-group of the ligand

the maxima in activity and enantioselectivity shift to different OH^- concentrations (see Tab. 4).

Table 4: Summary of the pKs values and OH^- concentration necessary for the highest TOF and ee of different ligands. The experimental error for the ee is ±1%.

Ligand	pKs	c(Base) [mM]	TOF_{max} [h^{-1}]	c(Base) [mM]	ee_{max} [%]
Prolin	10.60	60	97	40	39
Pipecolic acid	10.39	60	101	40	27
Alanin	9.87	30	138	40	20
Serin	9.15	30	12	30	7
Threonin	9.00	10	18	20	14

For PRO, which exhibits the highest pKs value of all investigated ligands, the highest ee was obtained with 40 mM OH^- and the highest TOF with 60 mM OH^-. Threonine, which exhibits the lowest pKs value required only 20 mM OH^- for the best ee and 10 mM OH^- for the highest TOF. This could be explained by the need of different concentration of OH^- to deprotonate the ligand and to ensure an effective binding to the surface. The binding concept for PRO can thus be transferred to other ligands. However, as shown it is necessary to optimize the functionalization conditions for each ligand in order to identify the best preparation conditions before catalytic performances are tested.

6.4 Structure-activity and Structure-selectivity Correlation in the Hydrogenation of a β-ketoester with PRO-Pt NPs

(Relevant paper: V)

A rational design of highly stereoselective ligand-functionalized heterogeneous catalyst can only be achieved if the underlying mechanistic details of the asymmetric control are elucidated. In Section 6.2 it was mentioned that the stereoselectivity is mainly determined by the ligand-reactant interaction, analogous to the basic principles of asymmetric homogeneous catalysis.[98] It thus seems reasonable, to test if general concepts from homogeneous catalysis may be transferable to ligand-functionalized NPs. In homogeneous catalysis the stereoselective control is mainly determined by steric and electronic interactions between the reactant and the chiral ligands.[19-21, 96]

Steric interactions, for example, steric attraction or steric hindrance and repulsion, can generate a restricted and privileged orientation of the reactant. In addition, attractive electronic interactions such as hydrogen bonding and/or π-π-stacking can fix the reactant in a confined orientation, favoring the formation of one of the two enantiomers.

Reactant and ligand structure were changed to determine their influence on the activity and the stereoselectivity and to develop an interaction model.[109] These studies were started with the hydrogenation of MAA the simplest β-ketoester. The keto group is catalytically hydrogenated while the ester-group can cause steric and/or secondary interactions. To clarify the role of the additional functional group, hydrogenation experiments have been performed for two further ketones of similar structures but without additional functional group (see Fig. 31).

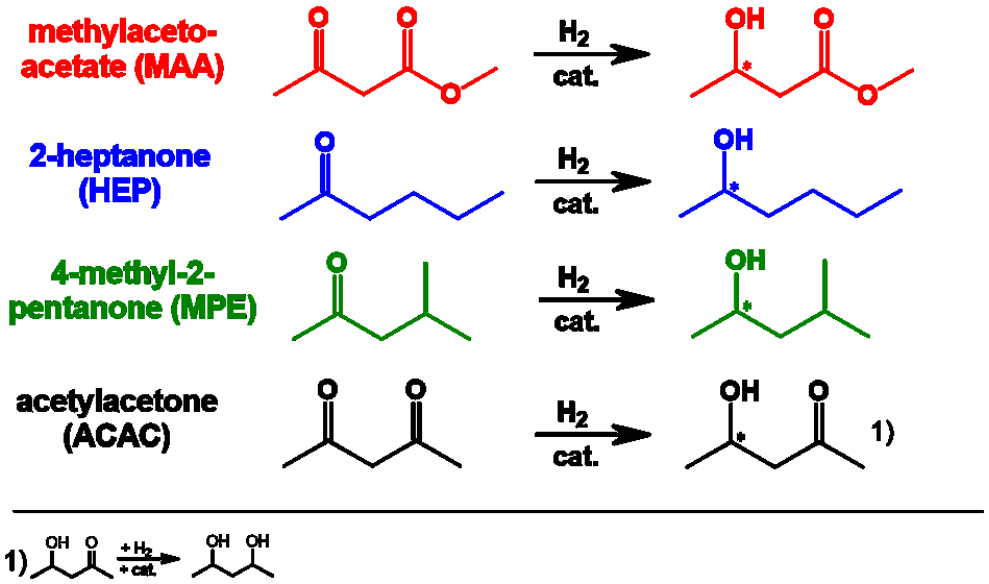

Figure 31: Studied catalytic hydrogenation reactions of different ketones. The different structures allow an empirical structure-activity and structure-selectivity investigation. Acetylacetone (ACAC) reacts in two hydrogenation steps. Here only the monohydrogenation is of interest.

The catalytic hydrogenation of these reactants (acetylacetone (ACAC) will discussed further below) over “ligand-free” and PRO-Pt NPs are shown in Figure 32.

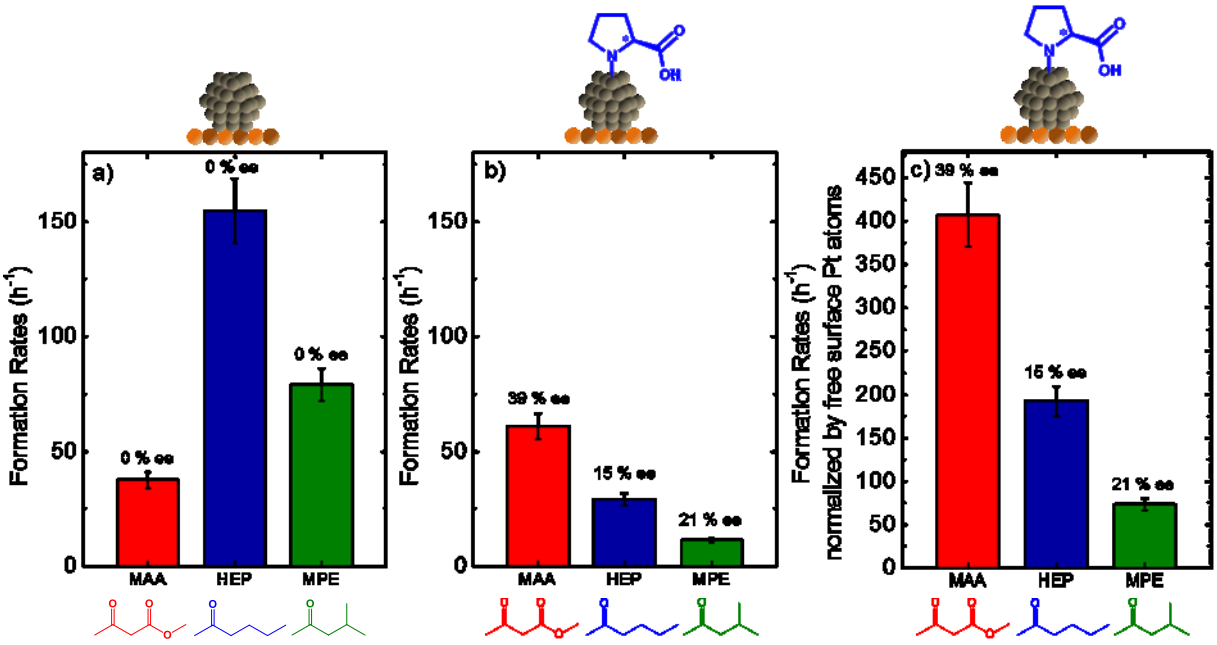

Figure 32: Formation rates normalized to the total number of Pt surface atoms and free surface Pt atoms for the hydrogenation reactions of the different ketones shown in Figure 31 (ACAC will discussed further below). The results for the reaction with "ligand-free" Pt are shown in a) and the results with PRO-Pt NPs are shown in b) and c). Enantioselectivites are shown as values above the bars. MAA shows by functionalizing the Pt NPs with PRO in contrast to HEP and MPE a significantly enhance rate. The experimental error for the ee is ±1%. All experiments were performed in autoclaves with 200 mg catalyst. The reaction pressure was 20 bar H_2, the reaction temperature 296 K and the stirring speed 800 rpm. For activity experiments 1 mL reactant and 9 mL dioxane was used and the conversion was kept below 10%. For ee experiments 0.5 mL methylacetoacetate and 4.5 mL dioxane was used.

The catalytic activities for the hydrogenation of 2-heptanone (HEP) and 4-methyl-2-pentanone (MPE) over "ligand-free" Pt NPs are significantly higher than that of MAA (see Fig. 32a). The linear HEP shows a 4 times higher and MPE a 2 times higher formation rate than MAA. As the steric demand of HEP and MPE is comparable to that of MAA, a possible explanation is that the smaller hydrogenation rate for MAA is related to the presence of the ester group that lowers the reactivity of the keto group. MPE has, in comparison to HEP a branched substituent. Increasing bulkiness near the reactive group lowers the accessibly of the keto group and so the adsorption on the metal surface is hindered, which leads to a decrease in activity.

The functionalization of the Pt NPs with PRO altered the activities significantly (see Fig. 32b). To discuss the rates of functionalized Pt NPs it has to be considered that only "ligand-free" surface atoms are involved in the hydrogenation reaction. Thus, the rates have to be normalized by the number of "ligand-free" surface atoms (see Fig. 32c).[57] This shows that the rate for MAA by functionalizing with PRO is strongly enhanced by a factor of ten. As discussed above this activity enhancement induced by PRO is related to a ligand acceleration effect ("N-H effect") induced by amine bound

hydrogen substituents.[84, 95-96] For HEP and MPE, the rates remain nearly constant upon functionalization with PRO. This indicates that the ester group plays an essential role for the activation and the resulting pronounced rate enhancement effect.

The changes in stereoselectivity over PRO-Pt NPs for MPE (21%) and HEP (15%) may be explained by small structural differences and resulting different steric interactions. In comparison, the enantioselectivity for MAA is significantly higher (39%). This suggests that also for the stereoselective control the ester group may be important. As HEP, MPE, and MAA exhibit similar steric demand the enhanced stereoselectivity for MAA is concluded to be related to an electronic interaction between the PRO ligand and the ester group of MAA.

PRO exhibits two functional groups, which are suitable to interact with the reactant: i) the amino, and ii) the carboxyl group. To identify the interacting group in PRO and to develop an interaction model, different amine ligands were investigated for the hydrogenation of MAA (see Fig. 33).

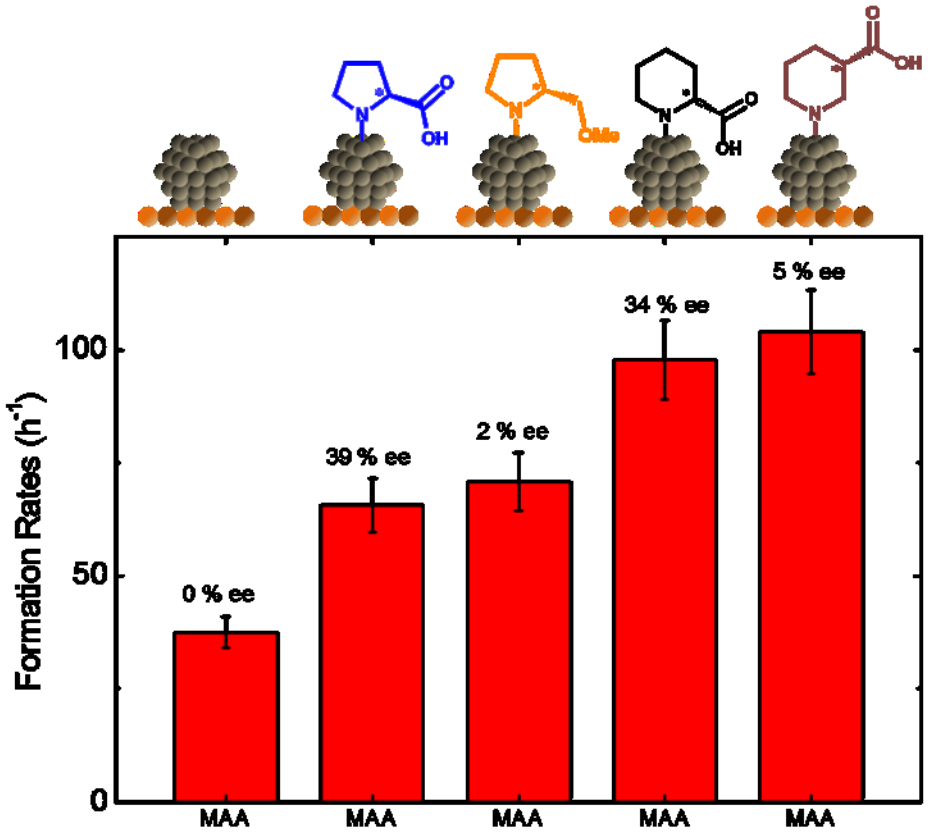

Figure 33: Formation rates and enantioselectivites for the hydrogenation of methylacetoacetate (MAA) with "ligand-free" and different ligand-functionalized Pt NPs (see top of diagram for catalyst structure). These results identify the relevance of kind and position of the functional group in the ligand. With PRO and Pipecolic acid significant enantioselectivies are achieved. The experimental error for the ee is ±1%. All experiments were performed in autoclaves with 200 mg catalyst, 1 mL methylacetoacetate, and 9 mL dioxane. The reaction pressure was 20 bar H_2, the reaction temperature 296 K, and the stirring speed 800 rpm. The conversion was kept below 10%.

All ligands, irrespective of the nature and position of their functional groups, show a rate enhancement compared to the “ligand-free” Pt NPs. For this effect, presumably, only the amino group is involved. For the asymmetric control, however, the position and the nature of the functional groups is important. Only with PRO and its 6-ring analogue high ees were achieved. Two types of interactions between the ester group and the PRO ligand can be determined from the influence of the ligand structure on the activity and selectivity:

1. The ester group interacts with the amine proton, leading to pronounced activation.
2. The ester group interacts with the carboxyl group, generating a strong asymmetric bias.

Based on these conclusions the two interaction models shown in Figure 34 can be postulated.

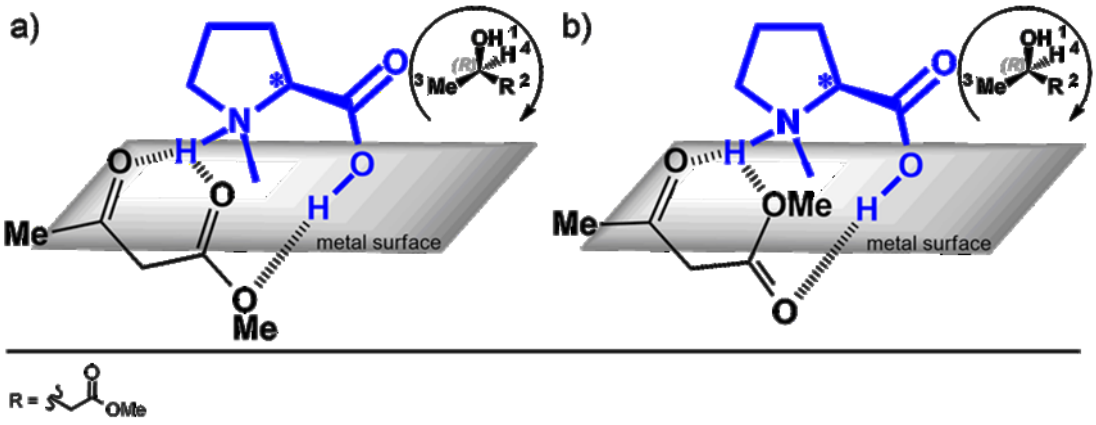

Figure 34: Interaction model proposed by the hydrogenation of different ketones over PRO-Pt NPs and the hydrogenation of methylacetoacetate with an ether-ligand. In addition to the interaction between the amino group of the ligand and the keto group of the reactant (“N-H effect”), the ester group of the reactant is involved in the activation (additional interaction). A further interaction between the ester (OMe (a) or C=O (b)) and the carboxyl proton of the ligand leads to a rigid 2-point binding.

The interaction modes lead to a so-called 2-point binding of the reactant with the ligand. As known from homogeneous catalysis, such bindings reduce the conformational flexibility and strengthen the asymmetric bias.[110]

In order to determine which part of the ligand actually interacts with the ester group and to validate which of the two models is more likely to describe the ligand-reactant interaction in Figure 34, ACAC was applied as a test reactant. ACAC exhibits two carbonyl groups, but no alkoxy substituent. Both carbonyl groups are reactive for hydrogenation leading to two reaction steps (see Fig. 31). For our purpose only the

first hydrogenation is of interest and the second step complicates determination of the activity. Because of that only the stereoselectivity for the product of the first hydrogenation step is discussed here. The stereoselectivity for ACAC is 20%. This result is similar to that obtained for MPE (21% ee, see Fig. 32) that exhibits a methyl group at the position where ACAC has the second keto group. In contrast, it differs significantly from the stereoselectivity achieved for MAA (39% ee) with the ester group in β-position. The carbonyl group in ACAC thus behaves rather like a methyl group and only steric interactions may influence the enantioselective control. This indicates that the alkoxy group of MAA is the interaction partner for the carboxyl group of PRO, leading to an enhanced stereoselective control. The mode on the left of Figure 34 is hence more likely to describe the interaction between MAA and PRO.

The different ligand structures show that a functional group in α-position is essential for stereoeselective control. The results for the hydrogenation of α-, β- and γ-ketoesters are shown in Figure 35.

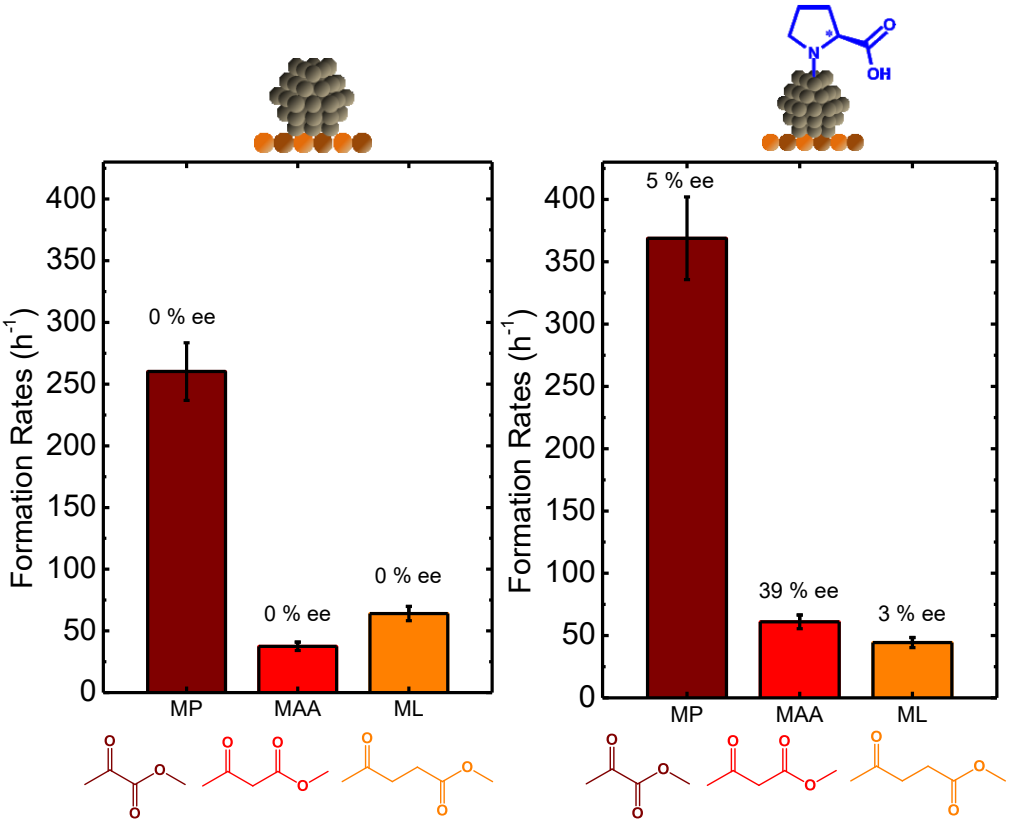

Figure 35: Formation rates for the hydrogenation of methylpyruvate (MP), methylacetoacetate (MAA) and methyllevulinate (ML) on "ligand-free" Pt NPs (left) and PRO-functionalized Pt NPs (right). The hydrogenation of MP and MAA show a significantly enhanced rate when using PRO-Pt NPs in comparison to "ligand-free" Pt NPs. Only with MAA an enantioselective control (39% ee) could be achieved. The experimental error for the ee is ±1%. All experiments were performed in autoclaves with 200 mg catalyst. The reaction pressure was 20 bar H_2, the reaction temperature 296 K, and the stirring speed 800 rpm. For activity experiments 1 mL reactant and 9 mL dioxane was used, and the conversion was kept below 10%. For ee experiments 0.5 mL reactant and 4.5 mL dioxane was used, and the experiments were run to full reactant conversion.

The hydrogenation of α-, β- and γ-ketoesters demonstrate that the position of the ester group influences the activity and enantioselectivity. Methylpyruvate (MP) shows a significantly higher formation rate for the hydrogenation over “ligand-free” Pt NPs then MAA and methyllevulinate (ML). This high formation rate can be attributed to the immediate proximity of the electron withdrawing ester group to the carbonyl group and a different steric demand. The same activity trend is observed for the hydrogenation of the three ketoesters over PRO-Pt NPs. The rates of MP and MAA show a rate enhancement by functionalizing with PRO compared to the “ligand-free” NPs (1.4 and 1.6 times higher activity). In case of ML, the activity decreases, but it has to be considered that only ligand-free surface atoms are contributed to the reaction. The decrease in rate enhancement from MAA, MP to ML may be attributed to the distance between the ester and the carbonyl group of the reactant. The distance in ML seems to be too long to facilitate participation of both groups in the reaction (see Fig. 36, ML is shown in the simplified staggered confirmation).

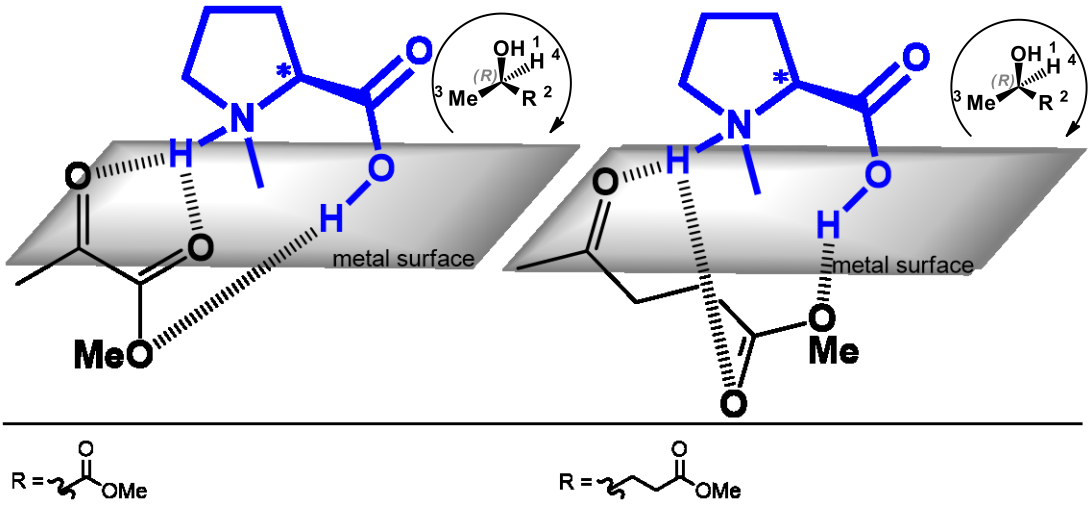

Figure 36: Possible interaction models for the rigid ligand-reactant interaction, between PRO-ligand and MP and ML reactant. Both reactants show no optimal interactions.

MP and ML show compared to MAA poor stereoselectivities (see Fig. 35). The longer or shorter distance between the ester and the keto group of the reactant causes a strong deviation from the optimal interaction mode between ligand and reactant. As a result, the desired 2-point binding mode is less likely to be formed, explaining the lower ees. This suggests that an ester group in α- or β-position is of importance for obtaining a pronounced ligand-acceleration effect, but a strong asymmetric bias is only achieved with a β-ketoester.

Using this interaction model, it should be suitable to predict the preferentially formed product configuration. Due to the binding with L-PRO, one enantiotopic faces (*si face*) of the carbonyl group of MAA is oriented towards the metal surface and the other one (*re face*) towards the reaction medium (see Fig. 37).

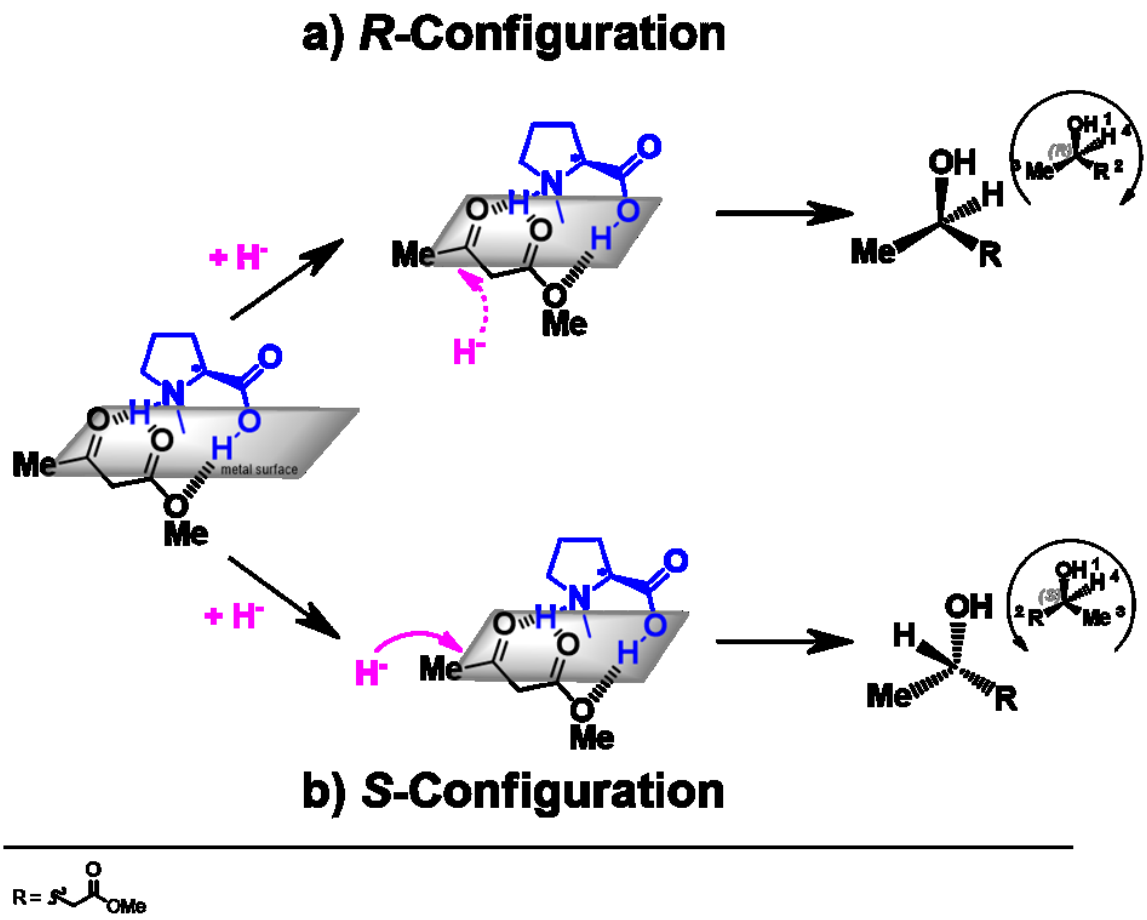

Figure 37: Hydrogenation pathways for methylacetoacetate on L-PRO-functionalized Pt. The more likely nucleophilic attack of H^- to the carbonly carbon from the metal side leads to the product with R-configuration (top). In contrast, forming the S-product from the proposed ligand-reactant interaction mode, requires a hydride attack on the reactant face that points towards the reaction medium.

The hydrogenation proceeds via hydride transfer from the metal surface to the prochiral C-atom and proton transfer from the amine to the O-atom.[98] As the hydride will preferentially attack the reactant at the face that points to the surface, the resulting alcohol should preferentially exhibit *R*-configuration. This proposing correlates with the experimental findings,[98] which further supports the postulated model.

6.5 Increase in Enantioselectivity by Controlling the Steric Demand of β-ketoesters

(Relevant paper: V)

In the previous section, it was shown that the control of enantioselectivity lies in the formation of a stabilized 2-point binding between the prochiral reactant and the chiral ligand.[109] This binding can be formed using a β-ketoester and an α-amino acid. In the following it is shown how the application of this model allows for further enhancing the enantioselectivity by a rational reactant choice.

Stereoselectivity is generated by the interaction of a prochiral reactant with a chiral ligand. This leads to two diastereotopic reaction pathways with different transition states of different free energies. The simplified assumption that the difference between the activation energies of these transition states determines the resulting ee is not valid, because both intermediates are quasi-equilibrated. Instead the ee is primarily determined by the difference in free activation energy *($\Delta\Delta G^{\ddagger}$)* of the respective two diastereomeric transition states (see Fig. 38), a phenomenon related to as the Curtin-Hammett principle. For this reason, the key to increase the ee is to stabilize the lower lying transition state and/ or to destabilize the higher lying transition state.[52]

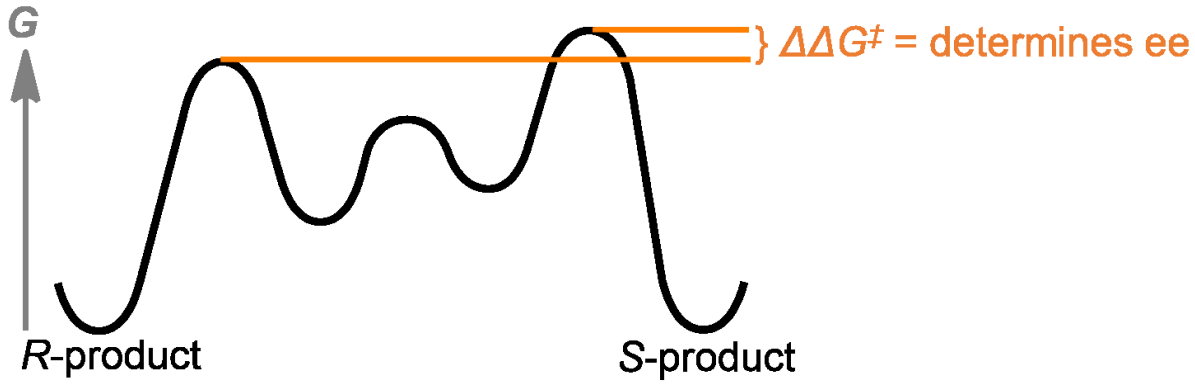

Figure 38: Schematic energy profile for the hydrogenation of MAA over PRO-Pt NPs. According to the Curtin-Hammett principle, the ee is determined by $\Delta\Delta G^{\ddagger}$. In our case it was experimentally shown that the R-product is preferentially formed.

The interaction mode in Figure 34a describes rather the adsorption complex, but not the transition state of the reaction. As the hydrogenation of ketones is highly exergonic, the adsorption state will closely reflect the transition state (Hammond's postulate).[111]

In the present case, the diastereotopic transition states that leads to the *R*-enantiomer should look like the binding mode illustrated on the left in Figure 34 and Figure 39. Its

diastereotopic counterpart is obtained by rotation 180° along the N-H bond. This binding leads to the product with the opposite configuration (S-enantiomer, see Fig. 39 on the right).

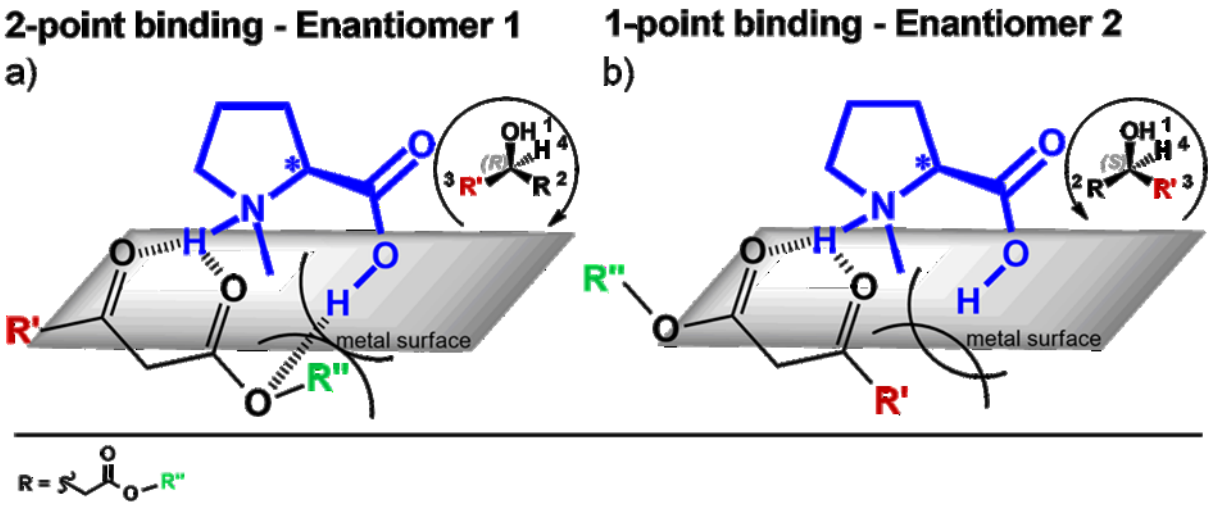

Figure 39: Different binding situations in the hydrogenation of a β-ketoester with PRO-Pt NPs. Beside the 2-point binding, which leads to the R- enantiomer, a 1-point binding is possible, leading to the S- enantiomer. The numbering of the alcohol conform to the Cahn-Ingold-Prelog convention.

Product analysis revealed that the product with *R*-configuration is the preferentially formed product. Thus, the transition state with the lower free activation energy has to be the one on the left of Figure 40. To increase the ee this transitions state has to be further stabilized or the transition state that leads to the *S*-product (Figure 40 right part) has to be destabilized.

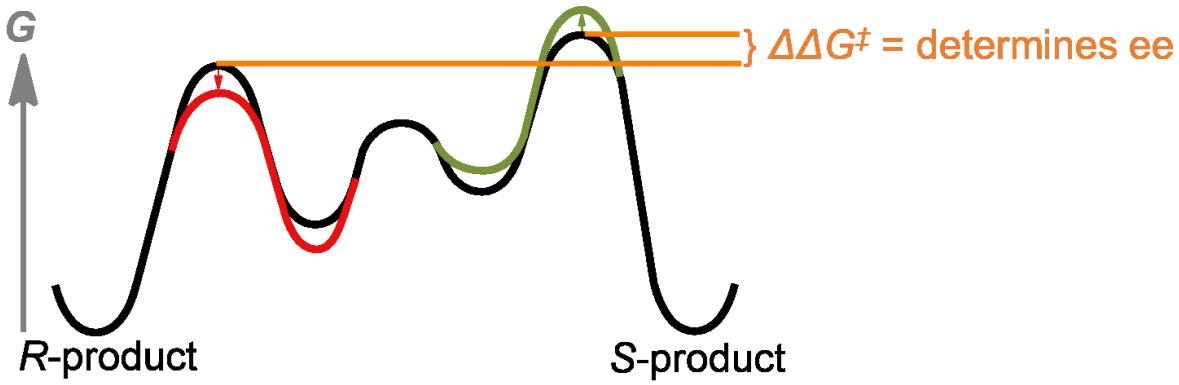

Figure 40: Energyprofile for the enantioselective hydrogenation of MAA over PRO-PT NPs. The difference in free activation energy (ΔΔG‡) determines the ees. The red curve represent the stabilizing of the desired 2-point binding and the green line the destabilizing of the undesired one-point binding, resulting both in an ee enhancement.

In homogeneous catalysis the key to enhance stereoselectivity is to manipulate the electronic and steric interactions.[21] The advantage of a pronounced electronic

interaction was already taken into account (see Fig. 39). Hence, steric interactions remain as the sole possibility to manipulate the free activation energies of the transition states. Therefore, the steric demand of the reactant's substituents was varied (see Fig. 41).

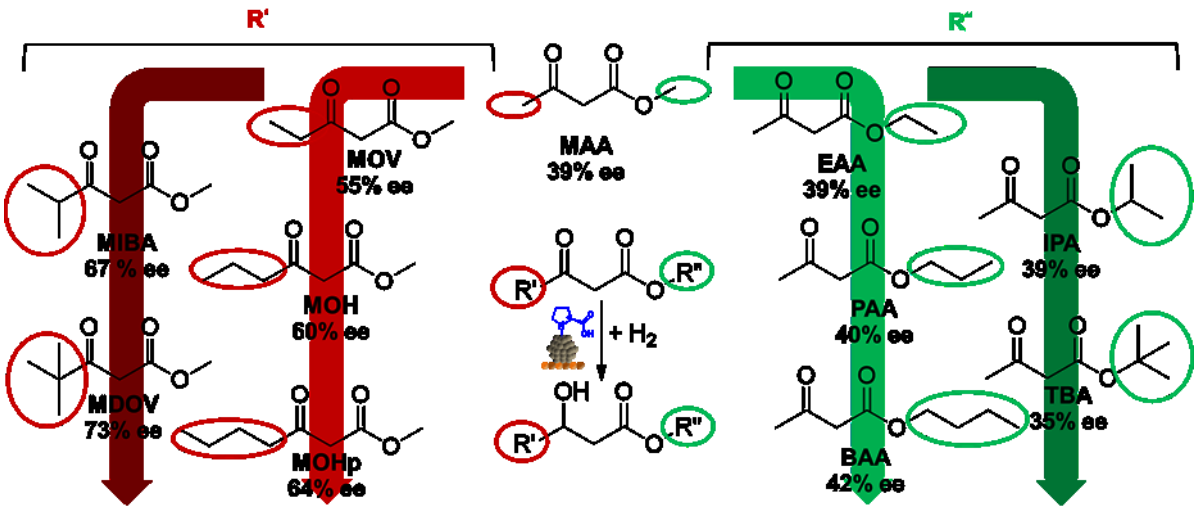

Figure 41: Enantioselectivities from various β-ketoesters with different chains tested in the hydrogenation with PRO-Pt NPs. By varying the steric demand of the reactant the enantioselectivity could be improved from 39% for MMA to 73% for MDOP. The experimental error for the ee is ±1%. All experiments were performed in autoclaves with 200 mg catalyst, 0.5 mL reactant, and 4.5 mL dioxane. The reaction pressure was 20 bar H_2, the reaction temperature 296 K, and the stirring speed 800 rpm. The experiments were run to full reactant conversion.

Changes of the alkyl chain on the ester side (R´´, green highlighted in Figure 41) should primarily effect the 2-point binding (see Fig. 39a). More steric demand will hinder the interaction between the reactant's alkoxy and the ligand's carboxyl group. As a result the desired 2-point binding mode is destabilized. An extension of the chain leads to a small improvement of ee from 39% for MAA to 42% for butylacetoacetate (BAA). Due to their flexibility, the alkyl substituents may rearrange to minimize repulsive steric interactions. However, if bulkier rigid groups with more steric demand are applied the ee eventually decreases to 35% (tert-butyl acetoacetate (TBA)), as these substituents cannot rearrange and thus destabilize the desired 2-point binding mode.

In contrast, if sterically more demanding groups are introduced on the other side of the reactant (R´, red highlighted in Figure. 41) the undesired 1-point binding mode (Figure 39b) is expected to be destabilized, which should lead to an improvement of the ee. Here already the extension of the chain length results in an increase of ee from 39% for MAA to 64% for methyl 3-oxoheptanoate (MOHp). A higher steric demand by introduction bulkier group leads to a further increase from 67% for methyl isobutyrylacetate (MIBA) to 73% for methyl 4,4-dimethyl-3-oxovalerate (MDOV).

This huge improvement is not only a new stereoselectivity record for supported ligand-functionalized NPs. It further demonstrates that general guiding principles from homogeneous catalysis can be transferred to supported catalysts. This reveals a yet unexplored potential to tune the catalytic properties of heterogeneous catalysts. Based on these encouraging results, it is her proposed that the functionalization of NPs with ligands will eventually allow for the design of asymmetric heterogeneous catalysts that should become competitive to tailored homogeneous catalysts.

7. Stability of Supported PRO-Pt NPs

(Relevant paper: V)

A heterogeneous catalyst is not soluble in the reaction medium. One significant economic and ecological advantage over homogeneous catalyst is, therefore, the possibility to recover the catalyst by filtration, as mentioned in the introduction. Experiments that were performed with PRO-Pt NPs previously showed that recycling does not alter the chemoselectivity, but the stereoselectivity decreases.[84] In Section 6.3 the catalyst preparation was optimized and in this way also the stereoselectivity. In order to investigate how the new catalyst preparation protocol affects the recyclability the recycling experiment have been repeated.[109]

PRO-Pt NPs were prepared by the new functionalization conditions and used for the hydrogenation of MAA (1st run). The catalyst were recovered by filtration after full conversion, dried at ambient conditions and again used as a catalyst (2nd run) for MAA hydrogenation. This recycling procedure was repeated a second time (3rd run). The two recovering cycles (see Tab. 5) reveal that the ees do not change significantly from the first run.

Table 5: Enantioselectivities for methylacetoacetate over PRO-Pt NPs (1st run) and recycled supported PRO-Pt NPs (2nd and 3rd run). The comparison of these results show that there is no significant change in ee, when the catalyst is recycled two times. All experiments were performed in autoclaves with 200 mg catalyst, 0.5 mL reactant, and 4.5 mL dioxane. The reaction pressure was 20 bar H_2, the reaction temperature 296 K, and the stirring speed 800 rpm. The experiments were run to full reactant conversion.

	1st run	**2nd run**	**3rd run**
ee (%)	39 ± 1	41 ± 1	40 ± 1

The new catalyst preparation protocol thus seems to generate more stable catalysts, which allows now a recycling without significant changes in stereoselectivity.

8. Conclusion

In the present work a synthetic approach was applied that allows for an independent control of the catalytically most relevant material properties (particle, ligand, and support). Stabile colloidal NPs were prepared without using any strongly binding surfactants. The surface chemistry of these NPs was analyzed using NMR and IR spectroscopy revealing that the particles are stabilized by CO and OH^-. Because the synthesis does not require strongly binding surfactants and both surface species, OH^- and CO, are easily replaced by more strongly binding molecules, these particles are referred to as “unprotected” NPs. “Unprotected” NPs can be used as building blocks to prepare tailored ligand-functionalized NPs.

Bare nanoparticles exhibit no chiral information. To achieve enantioselective hydrogenations of prochiral reactants a chiral element has to be introduced. In this work, the use PRO as a ligand was demonstrated to be particularly advantageous. The successful binding of PRO to the particle surface was confirmed by NMR-measurements. After deposition onto Al_2O_3 the supported ligand-functionalized NPs were used as heterogeneous catalyst for the hydrogenation of acetophenone. Catalytic investigation showed that PRO-Pt NPs, in comparison to “ligand-free” Pt NPs afford excellent chemoselectivities for the hydrogenation of the carbonyl group. Upon binding of PRO to the metal surface, these surface atoms are proposed to be blocked and ensembles of adjacent surface atoms are diluted. This suppresses the undesired hydrogenation of the phenyl ring. Although the binding of ligands blocks surface atoms the reaction rate was found to be enhanced when “ligand-free” NPs are functionalized with PRO. This increase in activity cannot be attributed to the blocking of large ensembles in favor of small ones. Instead a mechanism known from homogeneous catalysis as the “N-H effect” was concluded to proceed on PRO-Pt NPs. The hydrogen substituent at the amino group of PRO becomes acidic upon binding to Pt. This proton activates the reactant’s C=O group leading to an alternative reaction pathway with an enhanced rate over the purely metal catalyzed reaction.

The hydrogenation of acetophenone with PRO-Pt NPs gave a quite low ee of 14%. A significant improvement to 34% ee was achieved when changing the reaction to the hydrogenation of EAA. This value was sufficiently high to investigate the influence of particle size and ligand configuration on catalytic properties. It could be shown that the particle size alters only the activity but not the stereoselectivity. Also the ligand configuration has no influence on the absolute value of the ee. This suggests that the stereoselectivity does not depend on particle size, but it is determined by the ligand–reactant interaction.

To shed light onto the ligand-reactant interaction and to enhance stereoselectivities a structure-activity and structure-selectivity investigation was performed. By varying ligand and reactant, it could be shown that the combination of an α-amino acid and a β-ketoester results in a stabilized 2-point binding, which leads to an enhanced stereoselective control. The application of basic principles from asymmetric homogeneous catalysis to this model led to an increase of the ee to 73% by rational reactant choice.

The findings presented in this work demonstrate the ability to transfer principles from homogeneous to heterogeneous catalysis by functionalization of NPs with ligands. In this way, highly chemo- and stereoselective as well as stable catalysts can be designed. While in heterogeneous catalysis selectivity enhancements are usually accompanied by a loss of activity, the use of ligands was demonstrated to allow for improving activity and selectivity simultaneously. The application of ligands for supported catalysts hence serves as a novel approach with yet unknown potential to tune the catalytic performance of heterogeneous catalysts.

9. Outlook

The successful functionalization of Pt NPs with amino acids and derivatives as a promising novel approach for chemo- and stereoselective heterogeneous catalysis has been demonstrated in this work. The effective combination of the chemo- and stereoselective control could be shown recently for the hydrogenation of ethyl 3-oxo-3-phenylpropanoate (EOPP),[109] a β-ketoester with a phenyl substituent. These findings pave the way to a novel and more complex pool of reactants, being of interest as chiral building blocks for fine chemicals. Another interesting class of reactants that

will expand the pool of reactants, could be β-ketoamides, the analog to β-ketoesters, as this reactant class should also lead to the desired 2-point binding.

In order to confirm and get further evidence for the postulated ligand-reactant interactions ATR-IR spectroscopy in a reactor cell under reaction condition should be performed.

This work focused mainly on PRO as a ligand on Pt NPs. However, the here discussed results indicate that α-amino acids in general should be ideal ligands for β-ketoesters, because they lead to a 2-point binding between ligand and reactant.[109] Future studies may focus on further structural features. By small variations of the ligand and reactant structures improvements up to ees over 90% should be feasible. Interesting ligands are for example N-methyl-L-alanine and L-alanine. Recently, ligands that contain additional steric demand (L-2-phenylglycine and L-tert-Leucine) were investigated in the hydrogenation of β-ketoesters. Here stereoselectivities of more than 80% ee, the benchmark for industrial applications,[32] were obtained.

The results of the hydrogenation experiments revealed that functional groups in reactant and ligand are essential for high activities and stereoselectivities.[109] So far, however, the influence of the reaction solvent on the structural features has not been determined. It is known that β-ketoesters stand within a keto-enol equilibrium and hydrogenation of a C=C group proceeds faster than of a C=O group. With increasing polarity of the solvent the fraction of the keto form increases.[112-113] First tests showed that the solvent used for hydrogenation experiments influences the catalytic performance. It was observed that in general with increasing solvent polarity the activity decreases and the ee increases, this is consistent with the keto-enol equilibrium and the reactivities of both forms. To estimate and evidence the reactivity of both groups (C=O vs. C=C) 3-pen-2-one could be investigated.[114] Also the influence of the solvent should be systematically investigated by further hydrogenation experiments.

It has been shown that the steric demand on the carbonyl side of the reactant determines the stereoselective control (Section 6.5).[109] So far primary alkyl groups have been investigated. In tartaric acid-modified Raney nickel the introduction of a proper bulky group e.g. a cyclopropyl group in γ-position further increased the enantioselectivity.[38, 115] This reactant class should be investigated in more detail, e.g. with cyclopropyl, phenyl, 4-methylphenyl, 4-methoxyphenyl and 3,4-dimethoxyphenyl substituents in γ-position.

An aspect that thus far received only very limited attention is the support. Their acid-base properties may alter the catalytically performance. Depending on the surface chemistry the interaction between support and the ligand-shell can differ. This could significantly influence the stability of the particles on the support. Particle desorption may be inhibited even more effectively by using supports with other surface properties than γ-Al_2O_3, the standard support used within this work.

Furthermore, it could be shown that recycling experiments are possible without loss in stereoselective control. This raises another question: What is actually the maximal turnover number (TON)? To determine the maximal TON it would be necessary to generate continuous processes, which requires the development of a new reactor setup.

Bibliography

[1] R. A. Sheldon, I. W. C. E. Arends, U. Hansefeld, *Green Chemistry and Catalysis*, Wiley-VCH, **2007**.
[2] P. Anastas, N. Eghbali, *Chem Soc Rev* **2010**, *39*, 301-312.
[3] P. T. Anastas, M. M. Kirchhoff, *Accounts Chem Res* **2002**, *35*, 686-694.
[4] R. A. Sheldon, *Green Chem* **2007**, *9*, 1273-1283.
[5] I. Chorkendorff, J. W. Niemantsverdriet, *Concepts of Modern Catalysis and Kinetics*, Wiley-VCH, **2003**.
[6] S. Wnendt, K. Zwingenberger, *Nature* **1997**, *385*, 303-304.
[7] M. Reist, P. A. Carrupt, E. Francotte, B. Testa, *Chem Res Toxicol* **1998**, *11*, 1521-1528.
[8] E. J. Ariens, E. W. Wuis, E. J. Veringa, *Biochem Pharmacol* **1988**, *37*, 9-18.
[9] A. Shafaati, *Iran J Pharm Res* **2007**, *6*, 73-74.
[10] M. Reubold, R. Kempf, *CHEManager - Pharma & Biotech* **2016**, *1*, 3.
[11] I. Agranat, H. Caner, A. Caldwell, *Nat Rev Drug Discov* **2002**, *1*, 753-768.
[12] A. M. Rouhi, *Chem Eng News* **2003**, *81*, 56-61.
[13] N. M. Maier, P. Franco, W. Lindner, *J Chromatogr A* **2001**, *906*, 3-33.
[14] S. Erb, *Pharmaceutical Technology* **2006**, *30*, S14.
[15] H. U. Blaser, B. Pugin, F. Spindler, *J Mol Catal a-Chem* **2005**, *231*, 1-20.
[16] H. U. Blaser, F. Spindler, A. Studer, *Appl Catal a-Gen* **2001**, *221*, 119-143.
[17] H. U. Blaser, *Chem Commun* **2003**, 293-296.
[18] G. A. Somorjai, Y. G. Borodko, *Catal Lett* **2001**, *76*, 1-5.
[19] A. Borner, *Eur. J. Inorg. Chem.* **2001**, 327-337.
[20] M. Sawamura, Y. Ito, *Chem Rev* **1992**, *92*, 857-871.
[21] C. A. Tolman, *Chem Rev* **1977**, *77*, 313-348.
[22] W. S. Knowles, *Adv. Synth. Catal.* **2003**, *345*, 3-13.
[23] M. L. Crawley, B. M. Trost, **2012**.
[24] A. Ault, *J Chem Educ* **2002**, *79*, 572-577.
[25] I. V. Komarov, A. Borner, *Angew Chem Int Edit* **2001**, *40*, 1197-+.
[26] J. M. Hawkins, T. J. N. Watson, *Angew Chem Int Edit* **2004**, *43*, 3224-3228.
[27] U. Hintermair, G. Francio, W. Leitner, *Chem Commun* **2011**, *47*, 3691-3701.
[28] M. Heitbaum, F. Glorius, I. Escher, *Angew Chem Int Edit* **2006**, *45*, 4732-4762.
[29] J. Hagen, **1996**.
[30] P. Claus, *Top Catal* **1998**, *5*, 51-62.
[31] P. Maki-Arvela, J. Hajek, T. Salmi, D. Y. Murzin, *Appl. Catal., A* **2005**, *292*, 1-49.
[32] B. Pugin, H. U. Blaser, *Top Catal* **2010**, *53*, 953-962.
[33] S. Sabater, J. A. Mata, E. Peris, *Acs Catal* **2014**, *4*, 2038-2047.
[34] P. McMorn, G. J. Hutchings, *Chem Soc Rev* **2004**, *33*, 108-122.
[35] K. Ding, Y. Uozumi, **2008**.
[36] C. Li, *Catal Rev* **2004**, *46*, 419-492.
[37] A. Pfaltz, T. Heinz, *Top Catal* **1997**, *4*, 229-239.
[38] T. Sugimura, *Catal Surv Jpn* **1999**, *3*, 37-42.
[39] H. U. Blaser, H. P. Jalett, M. Muller, M. Studer, *Catal Today* **1997**, *37*, 441-463.
[40] T. Mallat, E. Orglmeister, A. Baiker, *Chem Rev* **2007**, *107*, 4863-4890.
[41] T. Osawa, T. Harada, O. Takayasu, *Top Catal* **2000**, *13*, 155-168.
[42] H. U. Blaser, H. P. Jalett, F. Spindler, *J Mol Catal a-Chem* **1996**, *107*, 85-94.
[43] H. U. Blaser, M. Studer, *Acc. Chem. Res.* **2007**, *40*, 1348-1356.

[44] R. Hess, A. Vargas, T. Mallat, T. Burgi, A. Baiker, *J Catal* **2004**, *222*, 117-128.
[45] T. E. Jones, C. J. Baddeley, *J Phys Chem C* **2007**, *111*, 17558-17563.
[46] P. Kukula, L. Cerveny, *Appl Catal a-Gen* **2001**, *210*, 237-246.
[47] T. Osawa, M. Onogi, I. Y. S. Lee, T. Harada, *React Kinet Mech Cat* **2011**, *103*, 443-449.
[48] N. Kunzle, R. Hess, T. Mallat, A. Baiker, *J Catal* **1999**, *186*, 239-241.
[49] Z. Ma, F. Zaera, *J Phys Chem B* **2005**, *109*, 406-414.
[50] H. Bonnemann, R. M. Richards, *Eur. J. Inorg. Chem.* **2001**, 2455-2480.
[51] S. Kunz, P. Schreiber, M. Ludwig, M. M. Maturi, O. Ackermann, M. Tschurl, U. Heiz, *Phys Chem Chem Phys* **2013**, *15*, 19253-19261.
[52] P. J. Walsh, M. C. Kozlowski, *Fundamentals of Asymmetric Catalysis*, University Science Books, **2009**.
[53] M. Campanati, G. Fornasari, A. Vaccari, *Catal Today* **2003**, *77*, 299-314.
[54] Y. Wang, J. W. Ren, K. Deng, L. L. Gui, Y. Q. Tang, *Chem Mater* **2000**, *12*, 1622-1627.
[55] J. Park, J. Joo, S. G. Kwon, Y. Jang, T. Hyeon, *Angew Chem Int Edit* **2007**, *46*, 4630-4660.
[56] V. K. Lamer, R. H. Dinegar, *J Am Chem Soc* **1950**, *72*, 4847-4854.
[57] J. Y. Park, C. Aliaga, J. R. Renzas, H. Lee, G. A. Somorjai, *Catal Lett* **2009**, *129*, 1-6.
[58] D. Astruc, F. Lu, J. R. Aranzaes, *Angew Chem Int Edit* **2005**, *44*, 7852-7872.
[59] C. Amiens, D. Decaro, B. Chaudret, J. S. Bradley, R. Mazel, C. Roucau, *J Am Chem Soc* **1993**, *115*, 11638-11639.
[60] M. Dasog, R. W. J. Scott, *Langmuir* **2007**, *23*, 3381-3387.
[61] R. Narayanan, M. A. El-Sayed, *Top Catal* **2008**, *47*, 15-21.
[62] M. P. Pileni, *J Phys Chem-Us* **1993**, *97*, 6961-6973.
[63] L. Dubau, C. Coutanceau, E. Garnier, J. M. Leger, C. Lamy, *J Appl Electrochem* **2003**, *33*, 419-429.
[64] W. X. Huang, Q. Hua, T. Cao, *Catal Lett* **2014**, *144*, 1355-1369.
[65] F. Fievet, J. P. Lagier, B. Blin, B. Beaudoin, M. Figlarz, *Solid State Ionics* **1989**, *32-3*, 198-205.
[66] I. Schrader, J. Warneke, S. Neumann, S. Grotheer, A. A. Swane, J. J. K. Kirkensgaard, M. Arenz, S. Kunz, *J Phys Chem C* **2015**, *119*, 17655-17661.
[67] C. Bock, C. Paquet, M. Couillard, G. A. Botton, B. R. MacDougall, *J Am Chem Soc* **2004**, *126*, 8028-8037.
[68] J. Yang, T. C. Deivaraj, H. P. Too, J. Y. Lee, *Langmuir* **2004**, *20*, 4241-4245.
[69] Z. Hens, J. C. Martins, *Chem Mater* **2013**, *25*, 1211-1221.
[70] Y. Y. Tong, C. Rice, N. Godbout, A. Wieckowski, E. Oldfield, *J Am Chem Soc* **1999**, *121*, 2996-3003.
[71] X. D. Wang, J. Stover, V. Zielasek, L. Altmann, K. Thiel, K. Al-Shamery, M. Baumer, H. Borchert, J. Parisi, J. Kolny-Olesiak, *Langmuir* **2011**, *27*, 11052-11061.
[72] P. Hollins, *Surface Science Reports* **1992**, *16*, 51-94.
[73] L. Altmann, S. Kunz, M. Baumer, *J Phys Chem C* **2014**, *118*, 8925-8932.
[74] B. A. Sexton, K. D. Rendulic, A. E. Hughes, *Surf Sci* **1982**, *121*, 181-198.
[75] A. F. Lee, D. E. Gawthrope, N. J. Hart, K. Wilson, *Surf Sci* **2004**, *548*, 200-208.
[76] F. M. Hoffmann, *Surface Science Reports* **1983**, *3*, 107-192.
[77] L. Kacenauskaite, J. Quinson, H. Schultz, J. J. K. Kirkensgaard, S. Kunz, T. Vosch, M. Arenz, *Chemnanomat* **2017**, DOI: 10.1002/cnma.201600313.
[78] E. Morsbach, M. Bäumer, S. Kunz, *unpublished results from PhD work*, **2014**.

[79] X. Y. Fu, Y. Wang, N. Z. Wu, L. L. Gui, Y. Q. Tang, *J Colloid Interf Sci* **2001**, *243*, 326-330.
[80] S. T. Marshall, M. O'Brien, B. Oetter, A. Corpuz, R. M. Richards, D. K. Schwartz, J. W. Medlin, *Nat Mater* **2010**, *9*, 853-858.
[81] K. R. Kahsar, D. K. Schwartz, J. W. Medlin, *J Am Chem Soc* **2014**, *136*, 520-526.
[82] D. Y. Petrovykh, H. Kimura-Suda, A. Opdahl, L. J. Richter, M. J. Tarlov, L. J. Whitman, *Langmuir* **2006**, *22*, 2578-2587.
[83] J. H. Ryu, S. S. Han, D. H. Kim, G. Henkelman, H. M. Lee, *Acs Nano* **2011**, *5*, 8515-8522.
[84] I. Schrader, J. Warneke, J. Backenkohler, S. Kunz, *J Am Chem Soc* **2015**, *137*, 905-912.
[85] S. Hauptmann, G. Mann, *Stereochemie*, Spektrum Akademischer Verlag, **1996**.
[86] M. Ellenberger, L. Pogliani, *Biochem Bioph Res Co* **1974**, *58*, 613-623.
[87] J. T. Scanion, D. E. Willis, *J Chromatogr Sci* **1985**, *23*, 333-340.
[88] T. Holm, *J Chromatogr A* **1999**, *842*, 221-227.
[89] C. Perego, S. Peratello, *Catal Today* **1999**, *52*, 133-145.
[90] C. T. Campbell, J. M. Campbell, P. J. Dalton, F. C. Henn, J. A. Rodriguez, S. G. Seimanides, *J Phys Chem-Us* **1989**, *93*, 806-814.
[91] A. Vargas, S. Reimann, S. Diezi, T. Mallat, A. Baiker, *J Mol Catal a-Chem* **2008**, *282*, 1-8.
[92] E. Bailon-Garcia, F. J. Maldonado-Hodar, A. F. Perez-Cadenas, F. Carrasco-Marin, *Catalysts* **2013**, *3*, 853-877.
[93] S. H. Pang, C. A. Schoenbaum, D. K. Schwartz, J. W. Medlin, *Nat Commun* **2013**, *4*.
[94] S. Puddu, V. Ponec, *Recl Trav Chim Pay B* **1976**, *95*, 255-257.
[95] S. E. Clapham, A. Hadzovic, R. H. Morris, *Coordin Chem Rev* **2004**, *248*, 2201-2237.
[96] R. Noyori, T. Ohkuma, *Angew. Chem., Int. Ed.* **2001**, *40*, 40-73.
[97] K. Abdur-Rashid, M. Faatz, A. J. Lough, R. H. Morris, *J Am Chem Soc* **2001**, *123*, 7473-7474.
[98] I. Schrader, S. Neumann, R. Himstedt, A. Zana, J. Warneke, S. Kunz, *Chem Commun* **2015**, *51*, 16221-16224.
[99] K. Schwetlick, *Organikum*, Wiley-VCH, **2001**.
[100] A. Cao, G. Veser, *Nat Mater* **2010**, *9*, 75-81.
[101] U. K. Singh, M. A. Vannice, *Appl Catal a-Gen* **2001**, *213*, 1-24.
[102] G. Ertl, M. Neumann, K. M. Streit, *Surf Sci* **1977**, *64*, 393-410.
[103] Y. L. Lam, J. Criado, M. Boudart, *Nouv J Chim* **1977**, *1*, 461-466.
[104] J. T. Wehrli, A. Baiker, D. M. Monti, H. U. Blaser, *J Mol Catal* **1989**, *49*, 195-203.
[105] A. Baiker, *J Mol Catal a-Chem* **1997**, *115*, 473-493.
[106] R. Noyori, T. Ohkuma, M. Kitamura, H. Takaya, N. Sayo, H. Kumobayashi, S. Akutagawa, *J Am Chem Soc* **1987**, *109*, 5856-5858.
[107] H. U. Blaser, H. P. Jalett, W. Lottenbach, M. Studer, *J Am Chem Soc* **2000**, *122*, 12675-12682.
[108] S. Neumann, S. Grotheer, J. Tielke, I. Schrader, J. Quinson, A. Zana, M. Oezaslan, M. Arenz, S. Kunz, **2017**, submitted.
[109] I. Schrader, S. Neumann, A. Šulce, F. Schmidt, V. Azov, S. Kunz, **2017**, submitted.
[110] N. Shibata, J. Kohno, K. Takai, T. Ishimaru, S. Nakamura, T. Toru, S. Kanemasa, *Angew Chem Int Edit* **2005**, *44*, 4204-4207.

[111] K. B. Wiberg, L. S. Crocker, K. M. Morgan, *J Am Chem Soc* **1991**, *113*, 3447-3450.
[112] M. Moriyasu, A. Kato, Y. Hashimoto, *J Chem Soc Perk T 2* **1986**, 515-520.
[113] S. G. Mills, P. Beak, *J Org Chem* **1985**, *50*, 1216-1224.
[114] S. Diezi, D. Ferri, A. Vargas, T. Mallat, A. Baiker, *J Am Chem Soc* **2006**, *128*, 4048-4057.
[115] S. Nakagawa, A. Tai, T. Okuyama, T. Sugimura, *Top Catal* **2000**, *13*, 187-189.

Curriculum Vitae

Persönliche Daten

Name:	Imke Schrader
Geburtsdatum:	04.07.1988 in Bremen
Kontakt:	Stieglitzstr. 21 28307 Bremen 0173 / 99 24 518 imke.schrader@uni-bremen.de

Akademische Ausbildung

12/2013 – vsl. 02/2017	Promotion, Universität Bremen, Deutschland Liebig-Stipendium des Fonds der chemischen Industrie „Ligandenfunktionalisierte Nanopartikel zur stereoselektiven, heterogenen Katalyse” bei Dr. S. Kunz am Institut für Angewandte und Physikalische Chemie
08/2013 – 11/2013	Forschungsaufenthalt, Universität Island, Island „The role of low energy electrons in focused electron beam induced deposition“ bei Prof. Dr. O. Ingólfsson
10/2010 – 03/2013	Master (Chemie), Universität Bremen, Deutschland Abschluss: Master of Science (Note 1,2)
10/2007 – 09/2010	Bachelor (Chemie), Universität Bremen, Deutschland Abschluss: Bachelor of Science (Note 2,0)

Schulische Ausbildung

08/2000 – 07/2007	Gymnasium Horn, Bremen, Deutschland Abschluss: Allgemeine Hochschulreife (Note 2,2)

Studienprojekte

09/2012 – 03/2013	Masterarbeit „Synthese, Cokristallisation und Oberflächenwachstum von aromatischen Phosphonsäuren und Imidazolderivaten“ bei Prof. Dr. P. Swiderek am Institut für Angewandte und Physikalische Chemie

01/2012 – 03/2012	Forschungspraktikum „Synthese, IR-Analyse und Elektronen-Bestrahlung von Kupferoxalat-SURMOFs“ bei Prof. Dr. P. Swiderek am Institut für Angewandte und Physikalische Chemie
10/2011 – 12/2011	Forschungspraktikum „Synthese und Charakterisierung von Tetrathiafulvalen-Cholesterol-Derivaten für die Immobilisierung in Vesikeln“ bei Priv.-Doz. Dr. V. Azov am Institut für Organische Chemie
06/2010 – 09/2010	Bachelorarbeit „Toxikologische Untersuchung von Bor-Clusern und Farbstoffen“ bei Prof. Dr. D. Gabel am Institut für Organische Chemie und Biochemie

Nebentätigkeiten

03/2013; 06/2013 – 10/2013	Studentische Hilfskraft, Universität Bremen, Institut für Angewandte und Physikalische Chemie, Prof. Swiderek
08/2010; 08/2011	Studentische Hilfskraft, Universität Bremen, Spurenanalytik, Prof. Balzer

Kenntnisse

Weiterbildung	MINT-Coaching 2009/2010	
Sprachen	Deutsch	Muttersprache
	Englisch	Erweiterte Kenntnisse
	Spanisch	Grundkenntnisse
	Russisch	Grundkenntnisse
	Latein	Kleines Latinum
EDV-Kenntnisse	Office-Anwendungen, Origin, EndNote	
Weiteres	Umfassende Sachkunde nach §5 der Chemikalien-Verbotsverordnung Führerschein der Klasse B	

Publications

1. I. Schrader, S. Neumann, A. Sulce, F. Schmidt, V. Azov, S. Kunz, Asymmetric Heterogeneous Catalysis – Transfer of Molecular Principles to Nanoparticles by Ligand Functionalization, **2017**, *submitted*.

2. S. Neumann, S. Grotheer, J. Tielke, I. Schrader, J. Quinson, A. Zana, M. Oezaslan, M. Arenz, S. Kunz, Nanoparticles in a Box: A Concept to Isolate, Store and Re-Use Colloidal Surfactant-Free Precious Metal Nanoparticles, **2017**, *submitted*.

3. I. Schrader, S. Neumann, R. Himstedt, A. Zana, J. Warneke, S. Kunz, The Effect of Particle Size and Ligand Configuration the Asymmetric Catalytic Properties of Proline-functionalized Pt-Nanoparticles, *Chemical Communications* **2015**, *51*, 16221-16224.

4. I. Schrader, J. Warneke, S. Neumann, S. Grotheer, A. A. Swane, J. J. K. Kirkensgaard, M. Arenz, S. Kunz, Surface Chemistry of “Unprotected” Nanoparticles: A Spectroscopic Investigation on Colloidal Particles, *Journal of Physical Chemistry C* **2015**, *119*, 17655-17661.

5. I. Schrader, J. Warneke, J. Backenköhler, S. Kunz, Pt Nanoparticles Functionalized with L-Proline – Achieving High Chemoselectivity with Enhanced Activity, *Journal of American Chemical Society* **2015**, *137*, 905-912.

6. D. Awad, M. Bartok, F. Mostaghimi, I. Schrader, N. Sudumbrekar, T. Schaffran, C. Jenne, J. Eriksson, M. Winterhalter, J. Fritz, K. Edwards, D. Gabel, Halogenated Dodecaborate Clusters as Agents to Trigger Release of Liposomal Contents, *ChemPlusChem* **2015**, *80*, 656-664.

7. U. Kauscher, K. Bartels, I. Schrader, V. A. Azov, B. J. Ravoo, Metastable oxidation states of tetrathiafulvalenes on the surface of liposomes, *Journal of Materials Chemistry B* **2015**, *3*, 475-480.

8. I. Schrader, L. Wittig, K. Richter, H. Vieker, A. Beyer, A. Gölzhäuser, A. Hartwig, P. Swiderek, Formation and Structure of Copper(II) Oxalate Layers on Carboxy-Terminated Self-Assembled Monolayers, *Langmuir* **2014**, *30*, 11945-11954.

9. S. Kunz, M. M. Maturi, I. Schrader, J. Backenköhler, M. Tschurl, U. Heiz, Same Ligand – Different Binding Mode: A Way to Control the Binding of N-acetyl-cysteine (NAC) to Pt Clusters, *Journal of Colloid and Interface Science* **2014**, *426*, 264-269.

10. D. Awad, I. Schrader, M. Bartok, N. Sudumbrekar, A. Mohr, D. Gabel, Brilliant Blue G as protective agent against trypan blue toxicity in human retinal pigment epithelial cells in vitro, *Graefes Archive for Clinical and Experimental Ophthalmology* **2013**, *251*, 1735-1740.

11. D. Awad, I. Schrader, M. Bartok, A. Mohr, D. Gabel, Comparative toxicology of trypan blue, brilliant blue G, and their combination together with polyethylene glycol on human pigment epithelial cells, *Investigative Ophthalmology & Visual Science* **2011**, *52*, 4085-4090.

Reprint of Publications

Publication II

Functionalization of Platinum Nanoparticles with L-Proline: Simultaneous Enhancements of Catalytic Activity and Selectivity

I. Schrader, J. Warneke, J. Backenköhler, S. Kunz

Journal of the American Chemical Society, **2015**, *137*, 905-912

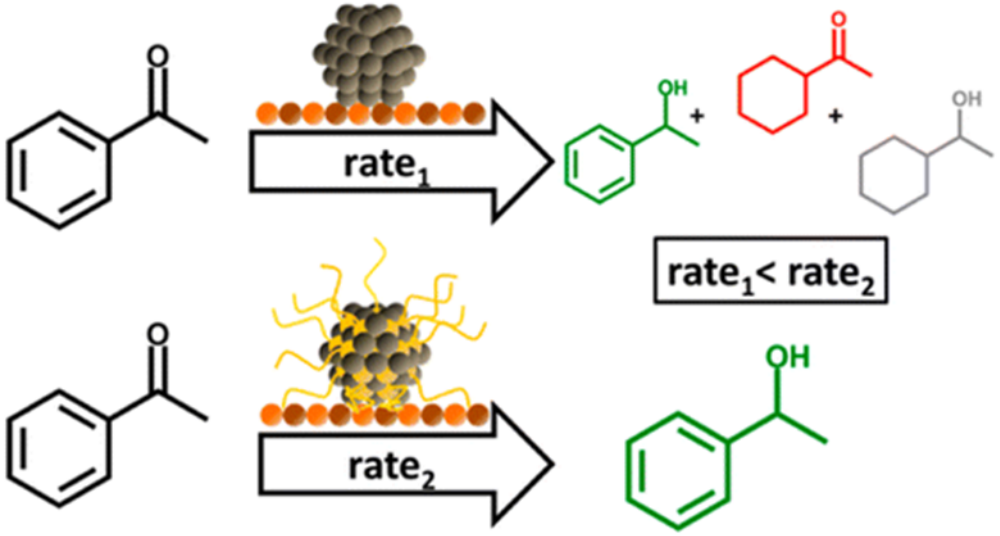

Publication III

Surface Chemistry of "Unprotected" Nanoparticles: A Spectroscopic Investigation on Colloidal Particles

I. Schrader, J. Warneke, S. Neumann, S. Grotheer, A. Abildgaard Swane, J. J. K. Kirkensgaard, M. Arenz, S. Kunz

The Journal of Physical Chemistry C, **2015**, *119*, 17655-17661

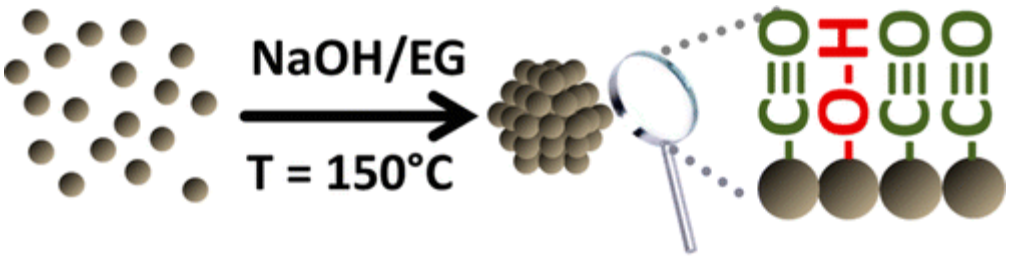

Publication IV

The Effect of Particle Size and Ligand Configuration on the Asymmetric Catalytic Properties of Proline-functionalized Pt-nanoparticles

I. Schrader, S. Neumann, R. Himstedt, A. Zana, J. Warneke, S. Kunz

Chemical Communications, **2015**, *51*, 16221-16224

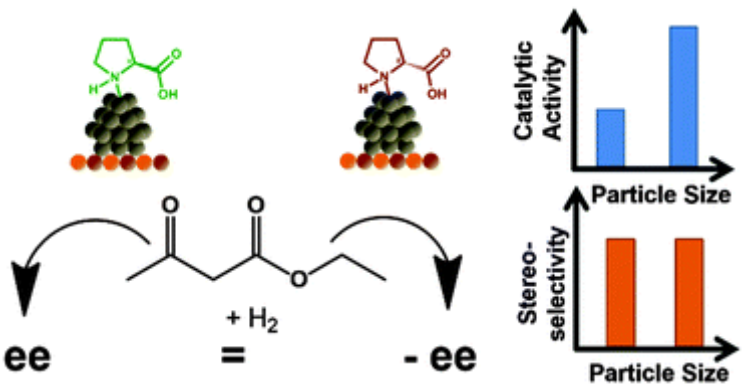

[98] – Reproduced by permission of The Royal Society of Chemistry.

Publication V

Asymmetric Heterogeneous Catalysis – Transfer of Molecular Principles to Nanoparticles by Ligand Functionalization

I. Schrader, S. Neumann, A. Sulce, F. Schmidt, V. Azov, S. Kunz

2017, *submitted*